Comprehensive Data Analysis for AMPT Tests on MO 740 and Hwy 54

December 2023
Final Report

Project number TR202417
MoDOT Research Report number cmr 23-017

PREPARED BY:

Jenny Liu

Yizhuang David Wang

Missouri University of Science and Technology

PREPARED FOR:

Missouri Department of Transportation

Construction and Materials Division, Research Section

TECHNICAL REPORT DOCUMENTATION PAGE

1. Report No. cmr 23-017	2. Government Accession No.	3. Recipient's Catalog No.
4. Title and Subtitle Comprehensive Data Analysis for AMPT Tests on MO 740 and Hwy 54		**5. Report Date** November 2023 Published: December 2023 **6. Performing Organization Code**
7. Author(s) Jenny Liu, Ph.D., P.E.; Yizhuang David Wang, Ph.D.		**8. Performing Organization Report No.**
9. Performing Organization Name and Address Department of Civil, Architectural and Environmental Engineering Missouri University of Science and Technology 1401 N. Pine St., Rolla, MO 65409		**10. Work Unit No.** **11. Contract or Grant No.** MoDOT project # TR202417
12. Sponsoring Agency Name and Address Missouri Department of Transportation (SPR-B) Construction and Materials Division P.O. Box 270 Jefferson City, MO 65102		**13. Type of Report and Period Covered** Final Report (April 2023-November 2023) **14. Sponsoring Agency Code**

15. Supplementary Notes

Conducted in cooperation with the U.S. Department of Transportation, Federal Highway Administration. MoDOT research reports are available in the Innovation Library at https://www.modot.org/research-publications.

16. Abstract

In this study, the S&T research team conducted comprehensive data analysis from the Asphalt Mixture Performance Tester (AMPT) samples collected in the Highway 54 and MO 740 projects. The MO 740 project in Boone County contained test sections with five mix designs, i.e., control mix, ground tire rubber (GTR)-modified mixture, and three mixtures containing recycled plastic. The Highway 54 project had ten samples collected at different times during the production of the surface mix. The data were analyzed on both the material and structural scales, and for the MO 740 project, field performance was also used to verify the research findings. The fatigue performance index S_{app} and the Rutting Strain Index (RSI) were calculated, and the mixture performance in pavement structures with realistic traffic loads and climate was predicted. The research found that the mixture performance in the Highway 54 project has a good correlation with the mixture volumetric properties. In terms of the different mix designs in the MO 740 project, the AMPT tests suggested that the GTR-modified mixture had the lowest modulus but had the highest cracking resistance. However, the mixture might have a higher rutting susceptibility than the other mixtures. On the other hand, the addition of plastic increased the mixture stiffness and did not have a great impact on the fatigue and rutting performance compared with the control mixture.

17. Key Words	18. Distribution Statement
Asphalt performance test; Fatigue; Rutting; Cracking resistance; Recycled plastic; Ground tire rubber; Field test	No restrictions. This document is available through the National Technical Information Service, Springfield, VA 22161.

19. Security Classif. (of this report)	20. Security Classif. (of this page)	21. No. of Pages	22. Price
Unclassified.	Unclassified.	51	

COMPREHENSIVE DATA ANALYSIS FOR AMPT TESTS ON MO 740 AND HWY 54

Prepared for

Missouri Department of Transportation

By

Jenny Liu, Ph.D., PE.

Yizhuang David Wang, Ph.D.

Department of Civil, Architectural and Environmental Engineering

Missouri University of Science and Technology

October 1, 2023

COPYRIGHT PERMISSIONS

DISCLAIMER

ACKNOWLEDGEMENTS

The authors wish to thank MoDOT for sponsoring this work. Special thanks go to Jacob Graessle and Daniel Oesch for the effort in data collection and technical support. The authors would also like to thank Ph.D. student Bo Lin for conducting the AMPT performance tests in the MO 740 project.

ABSTRACT

In this study, the S&T research team conducted comprehensive data analysis from the Asphalt Mixture Performance (AMPT) Tester samples collected in the Highway 54 and MO 740 projects. The MO 740 project in Boone County contained test sections with five mix designs, i.e., control mix, ground tire rubber (GTR)-modified mixture, and three mixtures containing recycled plastic, The Highway 54 project had ten samples collected at different times during the production of the surface mix. The data were analyzed on both the material and structural scales, and for the MO 740 project, field performance was also used to verify the research findings. The fatigue performance index S_{app} and the Rutting Strain Index (RSI) were calculated, and the mixture performance in pavement structures with realistic traffic loads and climate was predicted. The research found that the mixture performance in the Highway 54 project has a good correlation with the mixture volumetric properties. In terms of the different mix designs in the MO 740 project, the AMPT tests suggested that the GTR-modified mixture had the lowest modulus but also had the highest cracking resistance. However, the mixture might have a higher rutting susceptibility than the other mixtures. On the other hand, the addition of plastic increased the mixture stiffness and did not have a great impact on the fatigue and rutting performance compared with the control mixture.

EXECUTIVE SUMMARY

Missouri Department of Transportation (MoDOT) has been requiring the contractors to fabricate and submit Asphalt Mixture Performance Tester (AMPT) samples for performance testing as per Standards NJSP2001 and NJSP2108. Recently, the samples collected from the Highway 54 and MO 740 resurfacing projects have been tested by MoDOT and by Missouri University of Science and Technology (S&T), respectively. While the MO 740 project in Boone County contained test sections with five mix designs, i.e., control mix, ground tire rubber (GTR)-modified mixture, and three mixtures containing recycled plastic (polyethylene or PE), the Highway 54 project had ten samples collected at different times during the production of the overlay.

In this study, the S&T research team conducted comprehensive data analysis on the laboratory testing data. The data were analyzed on both the material and structural scales, and for the MO 740 project, field performance was also used to verify the research findings. On the material level, the fundamental material properties such as the dynamic modulus master curve, the ViscoElastic Continuum Damage (VECD) fatigue model, and the Shift rutting model parameters of the testing materials were obtained. Additionally, the material fatigue and rutting resistance indices, i.e., S_{app} and the Rutting Strain Index (RSI), were determined respectively in respect to the local Missouri climate conditions. The evaluation results were compared and correlated with the testing results from other performance testing methods. On the structural level, the fundamental material properties and the model coefficients were used to conduct the structural performance prediction in FlexPAVE™ with in-situ traffic volume and climate data. The performance deterioration of the pavement sections with respect to fatigue cracking was predicted as a function of service time. For the Highway 54 project testing data, the predicted performance was correlated with the measured volumetric-based acceptance quality characteristics (AQCs).

The research found that in the Highway 54 project the variability in production was well controlled in an acceptable range, according to the dynamic modulus and fatigue testing results. The performance-volumetric relationship (PVR) was successfully applied to the Highway 54 mixture. Using the PVR, the fatigue performance of mixtures produced for other sublots can be predicted once the volumetric information is measured during quality assurance (QA). In terms of the five mixtures used in the MO 740 project, the AMPT tests suggested that the GTR-modified mixture had the lowest modulus but also had the highest cracking resistance. However, the mixture might have a higher rutting susceptibility than the other mixtures. On the other hand, the addition of PE increased the mixture stiffness and did not have a great impact on the fatigue and rutting performance comparing with the control mix.

The field performance of the test sections on the Stadium Boulevard (MO 740) in Columbia, MO was extracted in this study. After eliminating the effects of field factors such as the traffic direction, it was found that the same trend was provided by the AMPT cyclic fatigue test and the IDEAL-CT cracking test.

TABLE OF CONTENTS

LIST OF FIGURES

LIST OF TABLES

LIST OF VARIABLES

Variable	Description	Equation Number
AMPT	Asphalt Mixture Performance Tester	-
SSR	Stress sweep rutting	-
GTR	Ground tire rubber	-
VECD	ViscoElastic Continuum Damage	-
S_{app}	Fatigue index parameter	-
RSI	Rutting Strain Index	-
AQCs	Acceptance quality characteristics	-
PVR	Performance-volumetric relationship	-
QA	Quality assurance	-
$\|E^*\|$	Dynamic modulus	(2.1)
a, b, d, and g	Model coefficients	(2.1)
f_R	Reduced frequency	(2.1)
E^*	The complex modulus	(2.2)
j	Complex number defined by $j^2 = -1$	(2.2)
ω	Angular frequency, $\omega = 2\pi f$, where f is the frequency	(2.2)
k, h	Two constants such that $0 < k < h < 1$	(2.2)
δ	A constant	(2.2)
E_{00}	The static modulus when ω tends towards 0	(2.2)
E_0	The glassy modulus when ω tends towards $+\infty$	(2.2)
η	The Newtonian viscosity of the dashpot, $\eta = (E_0 - E_{00})\beta\tau$	(2.2)
i	Characteristic time, whose value varies only with temperature	(2.2)
D^R	The failure criterion	(2.3)
α	Damage evolution coefficient	(2.3)
C_{11} and C_{12}	The damage characteristic curve model coefficients	(2.3)
a_T	The dynamic modulus shift factor shifting to the critical climate temperature of the region in consideration	(2.3)
VMA	Voids in mineral aggregate	-
VFA	Voids filled with asphalt	-
VMA_{IP}	The in-place VMA	(2.4)
V_a	The percentage of air void content at $N_{des.}$	(2.4)
$\%G_{mm}$	The compaction level as constructed	(2.4)
VFA_{IP}	In-place VFA	(2.5)

a, *b*, and *c*	Regression model coefficients	(2.6)
HWT	Hamburg Wheel Tracker	-
ARAN	Automatic Road Analyzer	-
ECR	Engineered Crumb Rubber	-
PE	Polyethylene	-
PCR	post-consumer	-
RET	Reactive Elastomeric Terpolymer	-
10ECR	Dry GTR mix, which used ECR product, included by 10% of virgin binder weight	-
50PE	Recycled PE mix, including 0.50% PE or PCR plastic by mix weight	-
25PE	PE mix, included by 0.25% of mix weight.	-
50PEL	50PE mix modified with 0.9% RET Compatibilizer, used as both a binder-plastic compatibilizer and elastomeric polymer	-

CHAPTER 1 INTRODUCTION

1.1 Problem Statement

Missouri Department of Transportation (MoDOT) has been requiring the contractors to fabricate and submit Asphalt Mixture Performance Tester (AMPT) samples for performance testing as per Standards NJSP2001 and NJSP2108. The AMPT performance tests, i.e., dynamic modulus, cyclic fatigue, and stress sweep rutting (SSR) tests, are the state-of-the-art testing methods that characterize the fundamental material properties. Recently, the samples collected from the MO 740 project have been tested by Missouri University of Science and Technology (S&T). The MO 740 project in Boone County contained test sections consisting of five mix designs, i.e., control mix, ground tire rubber (GTR)-modified mixture, and three mixtures containing recycled plastic.

In this study, the S&T research team conducted comprehensive data analysis on the laboratory testing data. Performance in the laboratory and predicted field performance of the innovative mixtures were analyzed and compared. In addition, the research team conducted similar analyses on the data collected from the HWY 54 project and investigated the impact of construction variability on pavement performance.

1.2 Study Objectives

The objective of the study is to process and perform comprehensive analyses on the AMPT testing data collected from the MO 740 and HWY 54 projects. The study analyzes the performance of the different mix designs in the MO 740 project on both the material and structural levels. The construction variability in the HWY 54 project is quantified by analyzing the AMPT testing data collected from the project.

1.3 Research Methods

The S&T research team processed the AMPT testing data collected in the MO 740 and the HWY 54 projects. The data include the dynamic modulus test, the cyclic fatigue test, and the SSR test. Table 1.1 presents the detailed information about the tests. The testing data on the MO 740 project were generated by the S&T team. The tests for the HWY 54 project were performed by MoDOT, and only the dynamic modulus and cyclic fatigue testing data were available.

Table 1.1 AMPT Performance Tests

Test	Num. of Replicates	Testing Method	Testing Results and Parameter
Dynamic Modulus	4	AASHTO TP 132	Dynamic modulus master curve, shift factors
Cyclic Fatigue	4	AASHTO TP 133	S_{app}; material integrity vs. damage accumulation curve, D^R fatigue damage criteria
SSR	4	AASHTO TP 134	RSI; permanent deformation at different temperatures, loading frequencies, and amplitudes

The research team analyzed the data on both the material and structural scales, and for the MO 740 project, field performance was also used to verify the research findings. On the material level, the data from AMPT dynamic modulus, cyclic fatigue, and SSR tests were first processed through the Excel-based FlexMAT™ program. The fundamental material properties such as the dynamic modulus master curve and the ViscoElastic Continuum Damage (VECD) fatigue model and the Shift rutting model parameters of the testing materials were obtained. Those material properties were the inputs to the structural performance analyses. Meanwhile, the researchers calculated the material fatigue and rutting resistance indices, i.e., S_{app} and the Rutting Strain Index (RSI), respectively, with the local Missouri climate conditions. The evaluation results were compared and correlated with the testing results from other performance testing methods.

On the structural level, the fundamental material properties and the model coefficients were used to conduct the structural performance prediction. The analysis used FlexPAVE™ with in-situ traffic volume and climate data. The performance deterioration of the pavement sections with respect to fatigue cracking was predicted as a function of service time. The performance of different materials in pavement structures was compared.

In terms of the HWY 54 data, since the samples were acquired from different construction sections, the structural performance analysis highlighted the impact of construction variability. The predicted performance was correlated with the measured volumetric-based acceptance quality characteristics (AQCs).

1.4 Report Layout

The report is composed of five chapters. Chapter 1 introduces the background of the study and the research methodology. Chapters 2 and 3 present the analysis of the data and findings from the Highway 54 project and the MO 740 project, respectively. Chapter 4 discusses field performance data collection and the comparison between lab testing results and field performance. In the end, the conclusions and recommendations are summarized in Chapter 5.

CHAPTER 2 COMPREHENSIVE DATA ANALYSIS FOR HIGHWAY 54 AMPT TESTS

2.1. Background

During the construction of the Highway 54 project, MoDOT collected asphalt loose mix samples. Ten samples, designated as 20CDSJL040 - 20CDSJL049, were acquired at different production time, representing the mixtures placed at different sublots. The collected loose mixtures were reheated in the laboratory and used to form performance testing specimens. The tests were designed to understand the variabilities during production and develop and revise the existing BMD and QA procedures.

2.2. Dynamic Modulus Data Analysis

The dynamic modulus tests on Samples 20CDSJL040 - 20CDSJL049 were performed at the MoDOT Central Laboratory and analyzed at S&T. The testing data were analyzed using the Microsoft Excel-based program FlexMAT™. Two dynamic modulus models, i.e., the Sigmoidal model and the 2S2P1D model, were applied in the analysis. Equations (2.1) and (2.2) present the mathematical forms of the two models. Both models can be used to construct the master curve of asphalt mixtures' dynamic modulus. While the Sigmoidal model consists of a simple symmetric curve, the 2S2P1D model is formed by a series of linear and nonlinear mechanistic elements, as presented in the schematic in Figure 2.1 (Kim et al. 2015, Kim et al. 2022).

$$\log\left|E^*\right| = a + \frac{b}{1+\frac{1}{e^{d+g*\log f_R}}} \tag{2.1}$$

where $|E^*|$ is the dynamic modulus, a, b, d, and g are model coefficients and f_R is the reduced frequency.

$$E^*_{2S2P1D}(\omega) = E_{00} + \frac{E_0 - E_{00}}{1 + \delta(j\omega\tau)^{-k} + (j\omega\tau)^{-h} + (j\omega\beta\tau)^{-1}} \tag{2.2}$$

Where E^* is the complex modulus, j is the complex number defined by $j^2 = -1$, ω is the angular frequency, $\omega = 2\pi f$, where f is the frequency, k, h are two constants such that $0 < k < h < 1$, δ is a constant, E_{00} is the static modulus when ω tends towards 0, E_0 is the glassy modulus when ω tends towards$+\infty$, η is the Newtonian viscosity of the dashpot, $\eta = (E_0 - E_{00})\beta\tau$ and τ is the characteristic time, whose value varies only with temperature.

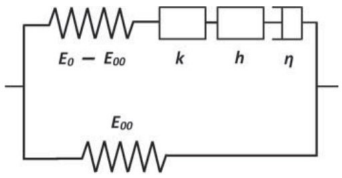

Figure 2.1 Schematic of the 2S2P1D model.

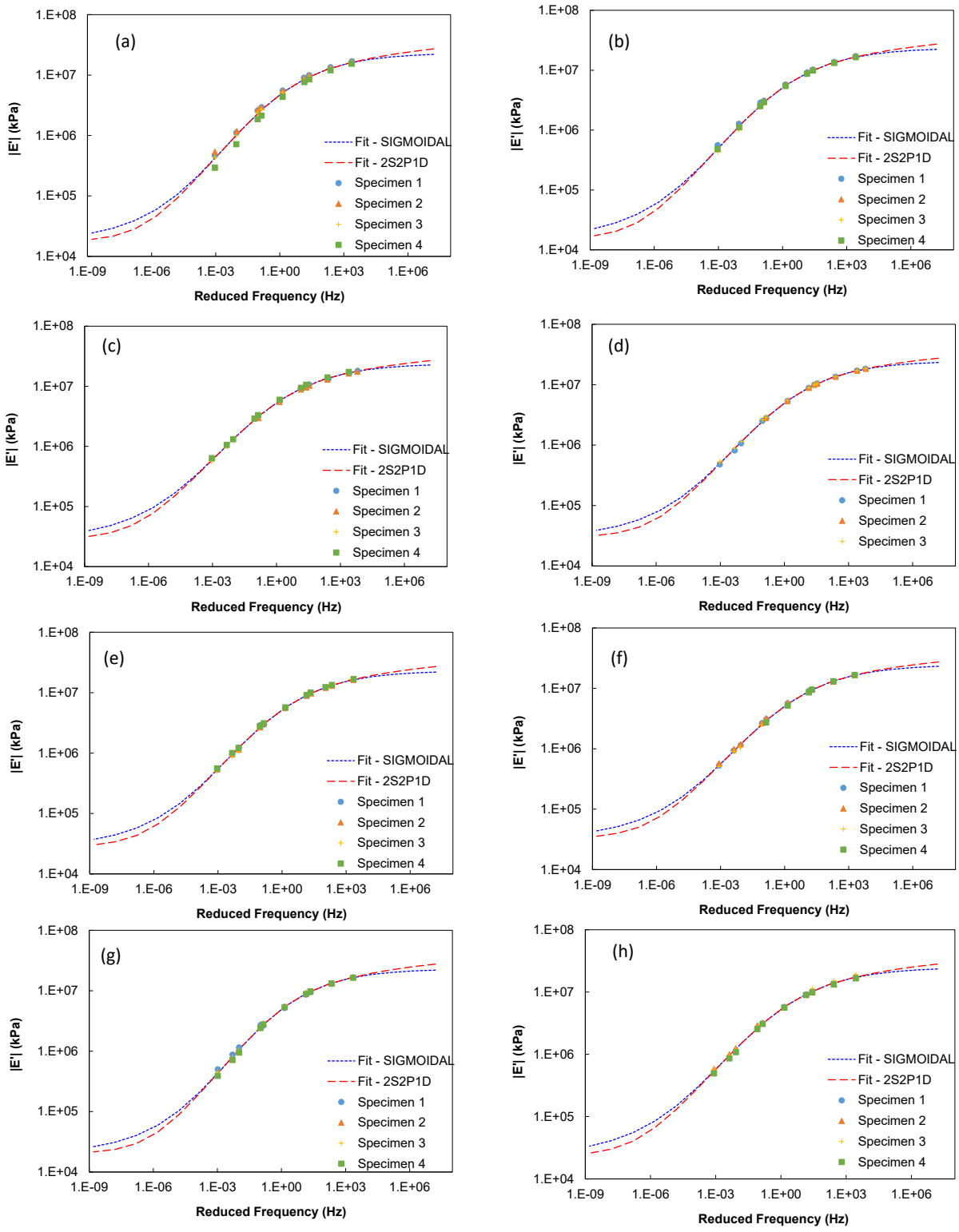

Figure 2.2 Dynamic modulus data of Highway 54 project: (a)-(f), Samples 040-045, and (g)-(h), Samples 048-049.

The dynamic modulus master curve of each sample is presented in Figure 2.2 while the data for Samples 046 and 047 were not available (presumably not tested due to sample fabrication issues). The results indicate that both the Sigmoidal function and the 2S2P1D model can well fit the dynamic modulus data that were measured at six frequencies and three temperatures. Within each sample, the repeatability among different specimens is high as indicated visually and statistically. The coefficients of variance (COV) of dynamic modulus and phase angle are presented in Appendix A. The values were calculated using the AASHTO T 378 method. The COV for dynamic modulus for all samples was lower than 8%, and the COV for phase angle was lower than 1.5%.

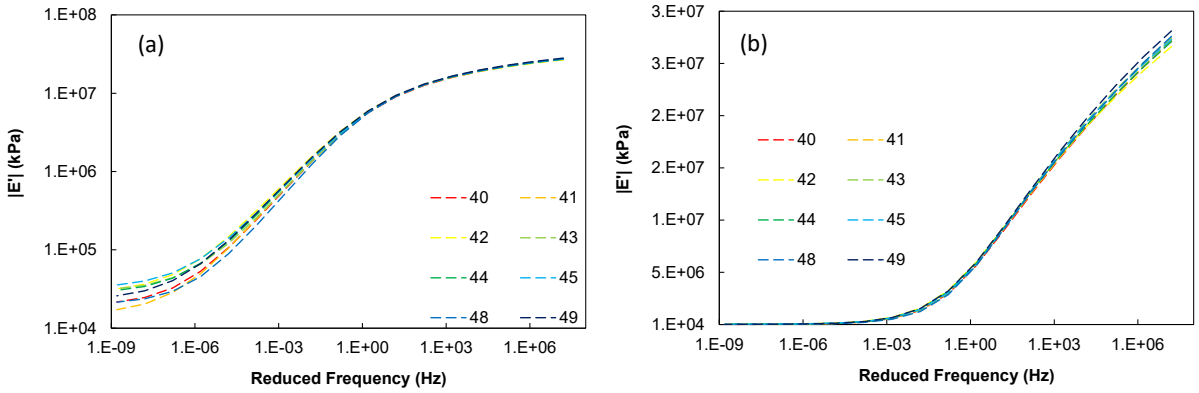

Figure 2.3 Dynamic modulus data of all samples: (a) in log-log scale, (b) in semi-log scale.

Figure 2.3 presents the overall comparison for the master curves for all the samples. The 2S2P1D model was used in this analysis. It can be observed that the fitted curves have highly overlapped each other. The modulus of different samples has similar values under the same frequency and temperature, especially on the high-frequency low-temperature region which is highlighted in the semi-log plot. Note that the tested samples are essentially one mixture produced at different production times. It can be concluded that some level of production and laboratory testing variability is observed but not significant. The finding also indicates that the contractor produced the mix in a relatively consistent manner throughout the construction. However, dynamic modulus is only one material property reflecting the material responses under small loading amplitudes; to further evaluate the impact of the production variability on pavement performance, different performance tests targeting different pavement distresses should be conducted.

2.3. Cyclic Fatigue Data Analysis

The cyclic fatigue tests in the Highway 54 project were performed as per AASHTO TP 133 at the MoDOT Central Laboratory, and the data were analyzed by S&T. The data were processed using the Microsoft Excel-based program, FlexMAT™, and the S-VECD model was used to interpret the results (Underwood et al. 2012, Wang and Kim 2017). The key component of the model is the energy-based damage characteristic curve or the C vs. S curve which describes the relationship between the material stiffness change and the accumulated damage. Each mixture has a unique C vs. S curve, regardless of the temperature, loading frequency, amplitude, and

loading history. Therefore, the C vs. S curve is a fundamental material property that can be used to predict the material fatigue damage evolution under complicated traffic loads.

The C vs. S curves of the ten samples are presented in Figures 2.4 and 2.5. Note that, since the dynamic modulus data for the Samples 046 and 047 were missing, the modulus of Sample 045 were used in their fatigue data analysis. It can be observed that the specimen-to-specimen variability within each sample was acceptable. Smooth C vs. S curves were generated for each sample. The ten curves were compared in Figure 2.6. The curves of different samples fell into a reasonable range, and no curve was significantly higher or lower than the others. Those C vs. S curves were used in the fatigue performance analysis.

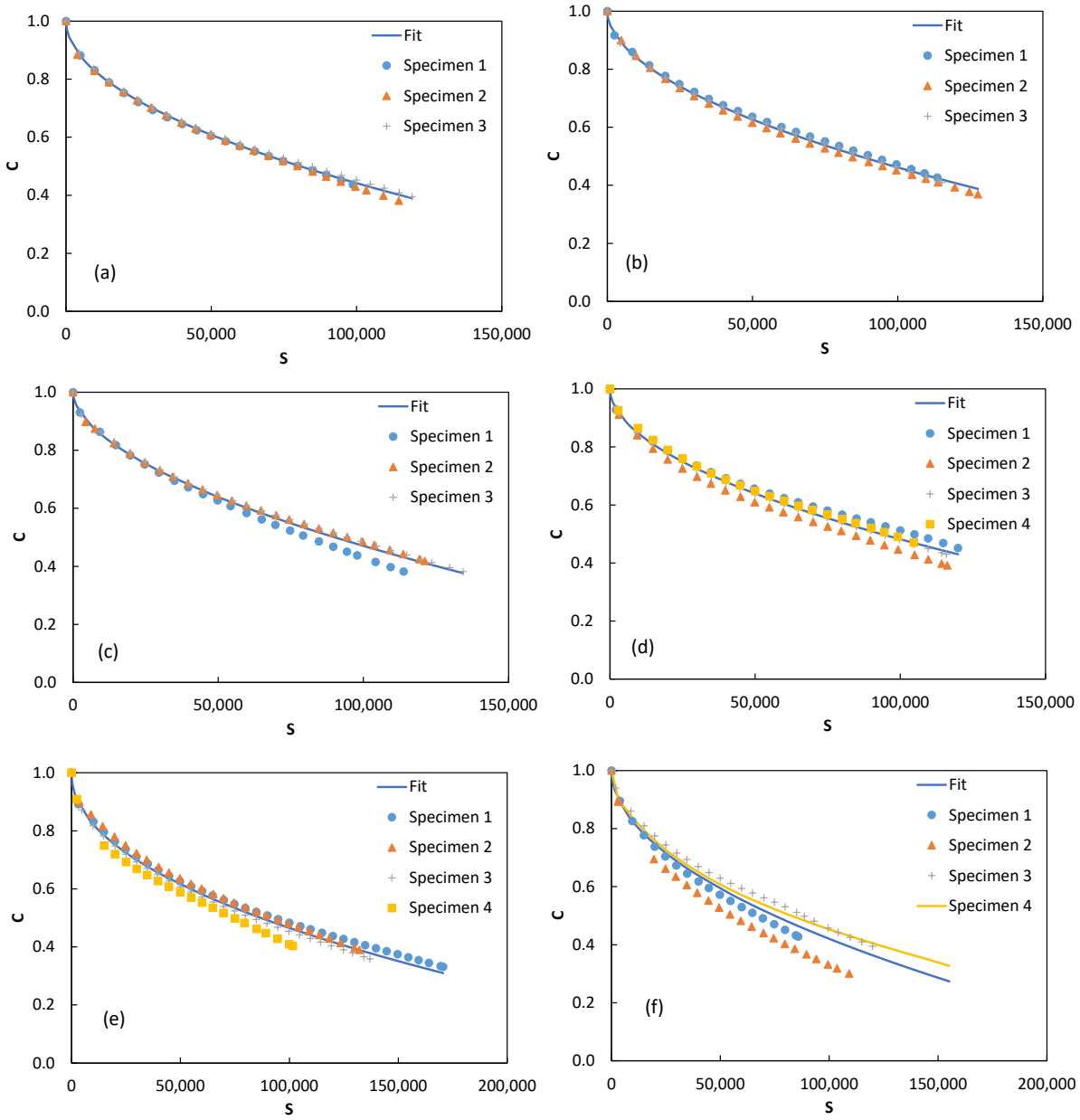

Figure 2.4 Damage characteristic curves for Highway 54 samples: (a) – (f), Samples 040 – 045.

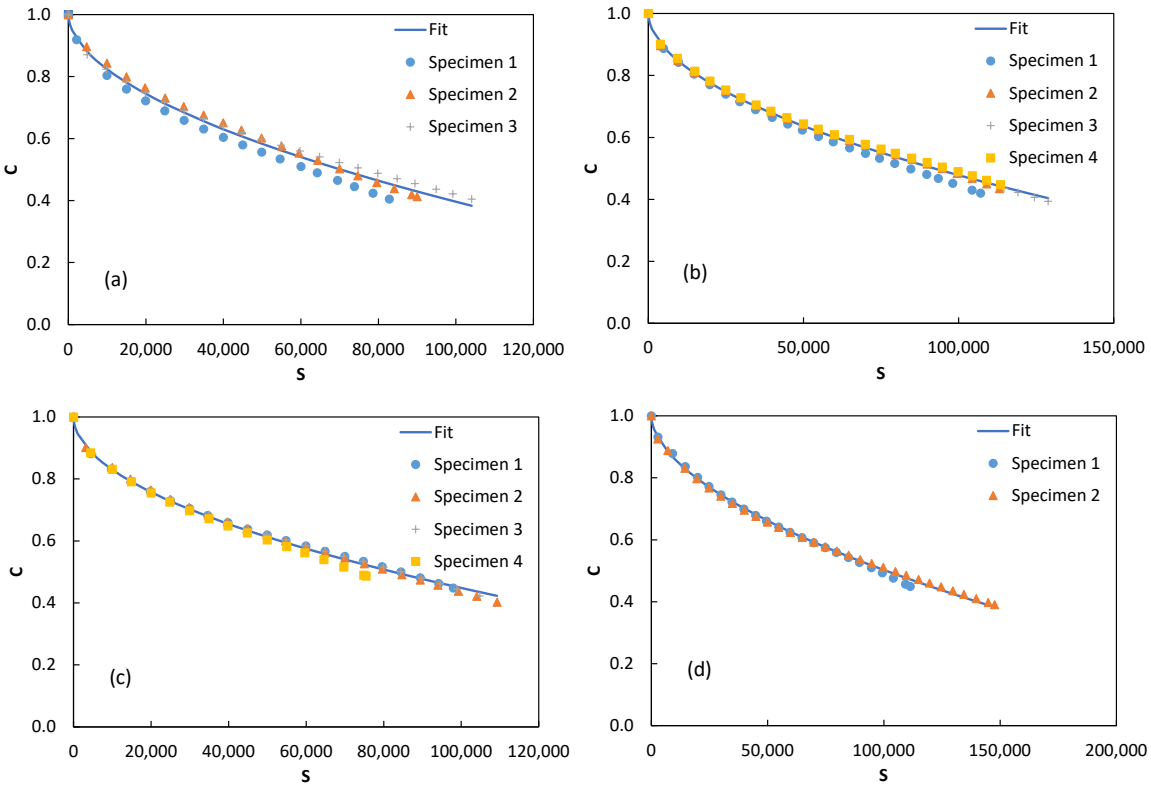

Figure 2.5 Damage characteristic curves for Highway 54 samples: (a) – (d) Samples 046 – 049.

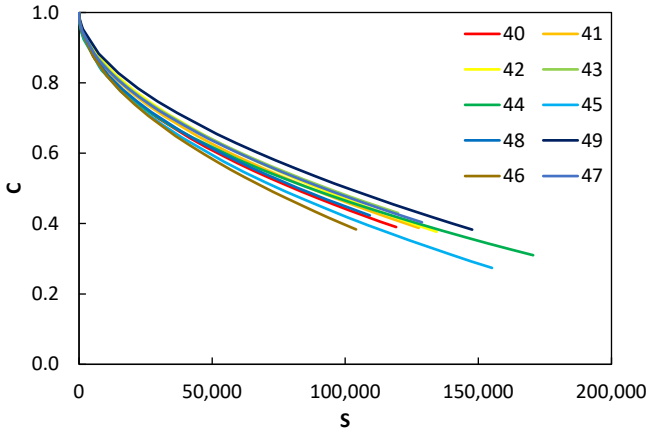

Figure 2.6 Overall comparison of the damage characteristics curves.

2.4. Fatigue Index Parameter Sapp

One effective method to evaluate the mixture's cracking resistance is using the fatigue index parameter, S_{app}. The parameter was developed by one of the authors at North Carolina State University based on the S-VECD model and has been utilized nationally since then (FHWA 2019, Wang et al. 2020,). Equation (2.3) shows the mathematical form of the parameter.

$$S_{app} = 1000^{\frac{\alpha}{2}-1} \frac{a_T^{\frac{1}{\alpha+1}} \left(\frac{D^R}{C_{11}}\right)^{\frac{1}{C_{12}}}}{\left|E^*\right|^{\frac{\alpha}{4}}} \tag{2.3}$$

where D^R is the failure criterion, α is the damage evolution coefficient, C_{11} and C_{12} are the damage characteristic curve model coefficients, a_T is the dynamic modulus shift factor shifting to the critical climate temperature of the region in consideration, and the $|E^*|$ is the dynamic modulus value of 10 Hz at the critical climate temperature. As indicated in the equation, the parameter considers the stiffness as well as the damage evolution potential of the mixture. A higher value of the S_{app} parameter means more resistance to fatigue cracking. Table 2.1 presents the S_{app} values of the sampled mixtures. According to the performance index, the cracking resistance of the mixtures laid in different sublots are relatively close with the high S_{app} value of 10.00 and low of 5.93.

Table 2.1 S_{app} Values of the Highway 54 Sample Mixtures

Sample ID	S_{app}
040	9.02
041	9.68
042	8.54
043	8.85
044	10.00
045	8.17
046	5.93
047	8.22
048	8.52
049	9.98

2.5. Correlation Between the Fatigue Performance and Volumetric Information

During production and conventional quality assurance (QA), only volumetric parameters are used to monitor the mix quality. To quantify the impact of volumetric change on mixture performance, a performance-volumetric relationship (PVR) was used by the FHWA in the Performance-Related Specification (Wang et al. 2019, Jeong et al. 2020, Kim et al. 2022). The PVR first combined the three variables, i.e., air void after field compaction, voids in mineral aggregate (VMA), and voids filled with asphalt (VFA) into two volumetric parameters, i.e., the in-place VMA (VMA_{IP}) and the in-place VFA(VFA_{IP}), as shown in Equations (2.4) and (2.5).

$$VMA_{IP} = 100 - \frac{\%G_{mm}}{100 - V_a} \times (100 - VMA) \tag{2.4}$$

$$VFA_{IP} = 100 - \frac{100 - \%G_{mm}}{VMA_{IP}} \times 100 \tag{2.5}$$

where V_a is the percentage of air void content at N_{des}, and $\%G_{mm}$ is the compaction level as constructed. The two volumetric parameters can further form a volumetric space, as presented in Figure 2.7, where one point in the space represents the volumetric condition of a mix design or the produced mixture. The volumetric space can be correlated with the performance of the mixture using a simple bilinear regression equation, as demonstrated in Figure 2.8 and Equation (6); in this case, the performance indicator is S_{app}.

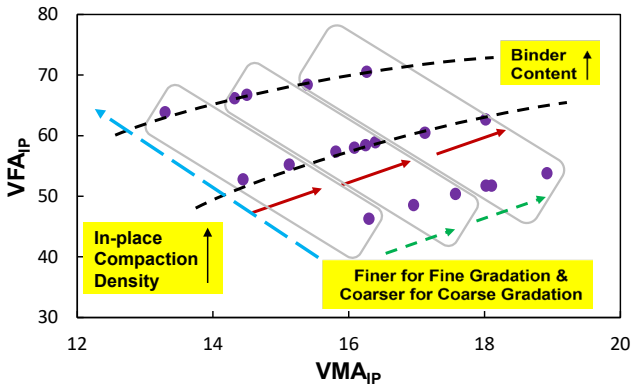

Figure 2.7 An example of the volumetric space of asphalt mixtures.

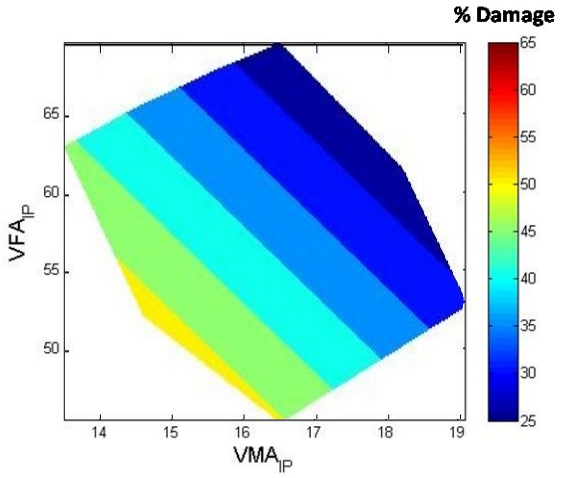

Figure 2.8 Example of fatigue damage contour in a volumetric space.

$$S_{app} = a \cdot VMA_{IP} + b \cdot VFA_{IP} + c \quad (2.6)$$

where a, b, and c are regression model coefficients.

Table 2.2 Volumetric Information of the Highway 54 Samples

ID	Design G_{mm}	Actual G_{mm}	Expected Void Content (%)	Actual Void Content (%)	Actual G_{mb}	Binder content (%)	VMA	VFA	Tested Avg AV	In-place VMA	In-place VFA
040	2.484	2.486	4.0	4.425	2.376	5.35	15.6	71.6	6.80	17.7	61.5
041	2.484	2.484	4.0	4.630	2.369	5.35	15.8	70.8	6.84	17.8	61.5
042	2.484	2.479	4.0	5.042	2.354	5.35	16.4	69.2	6.86	18.0	61.8
043	2.484	2.483	4.0	5.518	2.346	5.35	16.6	66.9	6.71	17.7	62.1
044	2.484	2.486	4.0	5.953	2.338	5.35	16.9	64.8	7.11	18.0	60.2
045	2.484	2.494	4.0	7.177	2.315	5.35	17.8	59.6	6.78	17.4	61.0
046	2.484	2.481	4.0	5.119	2.354	5.35	16.4	68.7	6.57	17.6	62.8
047	2.484	2.492	4.0	6.220	2.337	5.35	17.0	63.3	6.86	17.5	60.9
048	2.484	2.496	4.0	6.410	2.336	5.35	17.0	62.3	7.05	17.6	59.9
049	NA	NA	NA	NA	NA	NA	NA	NA	NA	NA	NA

The volumetric information of the Highway 54 samples is presented in Table 2.2, and their distribution in the volumetric space is presented in Figure 2.9. Note that the VMA_{IP} and VFA_{IP} are different than the commonly used parameters, VMA and VFA. The range of the variability for a produced mixture is acceptable. Using Equation (2.6), the PVR model coefficients were calibrated, and the regression results are presented in Figure 2.10. As shown in the figure, the model predicted S_{app} values of the samples are distributed close to the line of equality. It also indicates that, knowing the volumetric information from QA, the fatigue performance for mixtures in other sublots can be well predicted using the calibrated PVR.

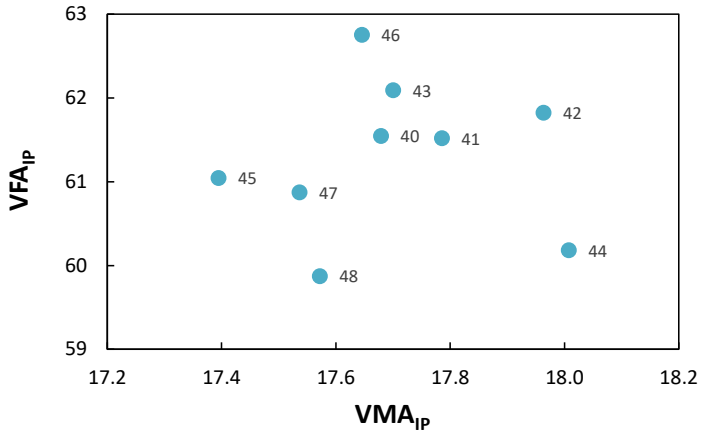

Figure 2.9 Volumetric distribution of the Highway 54 samples.

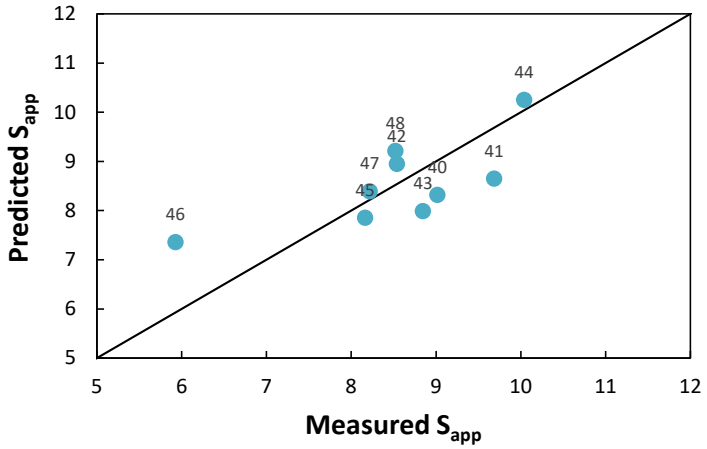

Figure 2.10 Predicted S_{app} from PVR vs. measured S_{app}.

2.6. Structural Performance Prediction Using FlexPAVE™

The merit of the AMPT tests is that they do not only provide performance thresholds to pass/fail the products, but also calibrate the fundamental mechanistic models that can be used in a full structural simulation that consider the in-situ pavement structure, traffic level, and realistic

climate conditions. In this study, the structure performance prediction was conducted in the finite-element based program, FlexPAVE™. The program utilized the fast Fourier transform to accelerate the calculation of pavement responses at different temperatures and integrated the S-VECD model and the Shift model for fatigue and rutting performance prediction, respectively (Wang et al. 2016, 2018, 2020).

In the structural simulation, the climate region was selected to be the Jefferson City area, and the traffic volume was set to be 13 million ESALs in 20 years based on the pavement design information. The pavement structure presented in Figure 2.11 was used. The actual construction plan in this project was a mill and fill asphalt overlay on top of existing concrete layers. Since FlexPAVE™ is not ready to predict reflective cracking on asphalt-concrete overlays, a typical 4" asphalt pavement structure was used in the demonstration to highlight the differences in the predicted fatigue damage among different sublots.

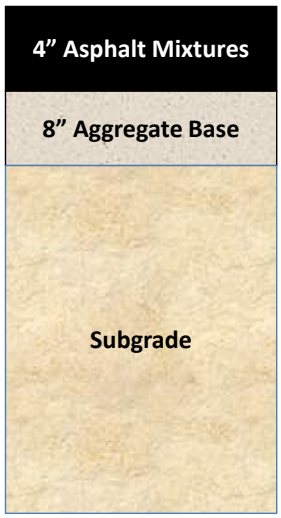

Figure 2.11 Schematic of pavement structure used in FlexPAVE™ performance simulation.

The predicted pavement damage is presented in Figure 2.12. The damage grows as the traffic loads are consistently applied in the 20 years of the design life. The amount of damage varies among the samples from different sublots between 18% to 25% at the end of the service life. If only 20% damage in the asphalt layer is allowed in pavement design, disincentives may be issued in this case. In addition, the trends in the predicted pavement damage and in the material performance index are consistent. For instance, while Sample 046 has the lowest S_{app} value, the simulation predicts that the sublot has the highest damage among all the sections. Figure 2.13 presents the damage distributions of the most and least damaged sections within the asphalt layer cross sections at the end of the design life.

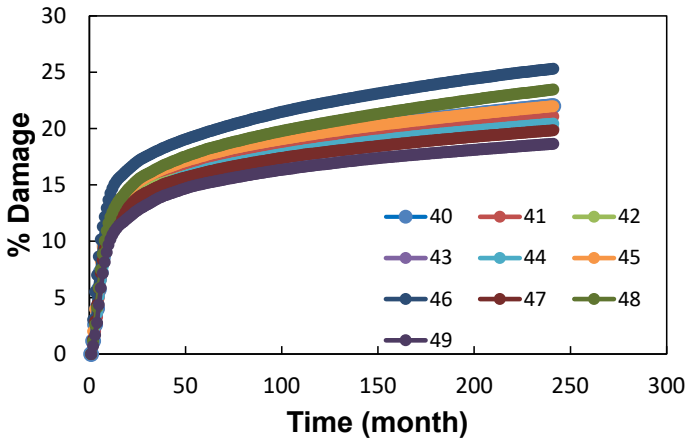

Figure 2.12 Predicted fatigue damage growth in different sublots.

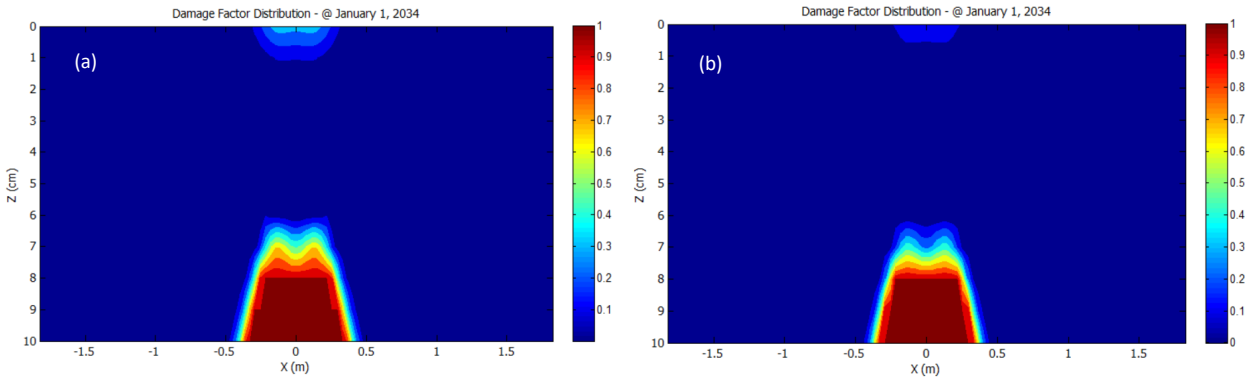

Figure 2.13 Fatigue damage contours within a pavement cross-section in asphalt layers: (a) Sample 46 and (b) Sample 49.

2.7. Summary

In this study, the AMPT testing data from the dynamic modulus test and the cyclic fatigue tests on the Highway 54 samples were analyzed. The sample quality and their cracking resistance were evaluated on both the material and structural levels. The findings are summarized as follows.

- The dynamic modulus master curves were constructed using the Sigmoidal and the 2S2P1D models. The specimen-to-specimen testing variability was acceptable, and the mixes produced at different times were relatively consistent in terms of mixture stiffness.

- The fatigue damage characteristic curves of different samples for the Highway 54 mixture falls into reasonably close range, indicating the variability in production exists but was controlled in an acceptable range.

- The fatigue index parameter, S_{app}, was used to evaluate the mixture cracking resistance. According to the performance index, the cracking resistance of the mixtures laid in different sublots are relatively close with the high S_{app} value of 10.00 and low of 5.93.

- The PVR function was successfully applied to this mixture. Using the PVR, the fatigue performance of mixtures produced for other sublots can be predicted once the volumetric information is measured during QA.

- In the structural performance simulation, the damage growth, and the amount of damage at the end of pavement life on different sublots were predicted. The percentage damage in asphalt layers varied between 19% to 25% due to the production variability. The ranking of the samples was consistent with the ranking of the material-level cracking resistance index.

CHAPTER 3 COMPREHENSIVE DATA ANALYSIS FOR MO 740 (STADIUM BOULEVARD) AMPT TESTS

3.1. Background

In August 2021, the Stadium Boulevard in Columbia, MO (Route 740) was resurfaced, and 1.64 miles of the project was used as test sections paved with four innovative asphalt mixtures to evaluate their field performance. The information of the newly designed mixtures is presented in Table 3.1. The layout of the test sections is presented in Figure 3.1. The rest of the Stadium Boulevard was paved with a SP095C hot mix asphalt (HMA) serving as the control. During the construction, loose mixtures were sampled, and performance tests, including the IDEAL-CT cracking test, the Hamburg Wheel Tracker (HWT) rutting test, and the AMPT tests were conducted. The IDEAL-CT and the HWT tests were performed by University of Missouri, Columbia (Mizzou). The IDEAL-CT tests were conducted with two conditions, i.e., samples compacted on site during production and samples compacted after reheated in the asphalt laboratory. The AMPT dynamic modulus test, cyclic fatigue test, and the stress sweep rutting (SSR) test were conducted at S&T in Summer 2022.

Table 3.1 Information of the Mixtures Used in the Stadium Boulevard Resurface Project.

Sample ID	Designation	Design
21M1V006 - V011	Control	SP095C HMA
21M1V012	10ECR	Dry process ground tire rubber (GTR) mix, which used an Engineered Crumb Rubber (ECR) product, included by 10% of virgin binder weight.
21M1V013	50PE	Recycled Polyethylene (PE) mix, including 0.50% PE or post-consumer (PCR) plastic by mix weight.
21M1V014	25PE	PE mix, included by 0.25% of mix weight.
21M1V015	50PEL	50PE mix modified with 0.9% Reactive Elastomeric Terpolymer (RET) Compatibilizer, used as both a binder-plastic compatibilizer and elastomeric polymer.

Figure 3.1 Demonstration project layout (Rath et al. 2022)

3.2. Dynamic Modulus Testing Data of the MO 740 Project

The dynamic modulus of all the testing samples on MO 740 are presented in Figure 3.2. In Figure 3.2 (a), the master curves of all the six samples for the control SP095C mixture are plotted, and it shows except Sample V009, all the master curves are overlapping on each other. While the samples were collected at different time during production, the sample-to-sample variability is low. Figure 3.2 (b) presents the master curves of the testing mixtures with a representative control mixture master curve from Sample V007. While the 50PE mixture has the highest modulus, the 10ECR mix exhibited the lowest. The 25PE and 50PEL mixtures tend to have similar modulus with the control mixture. It is expected that a high content of polyethylene increases the stiffness of the asphalt mixture.

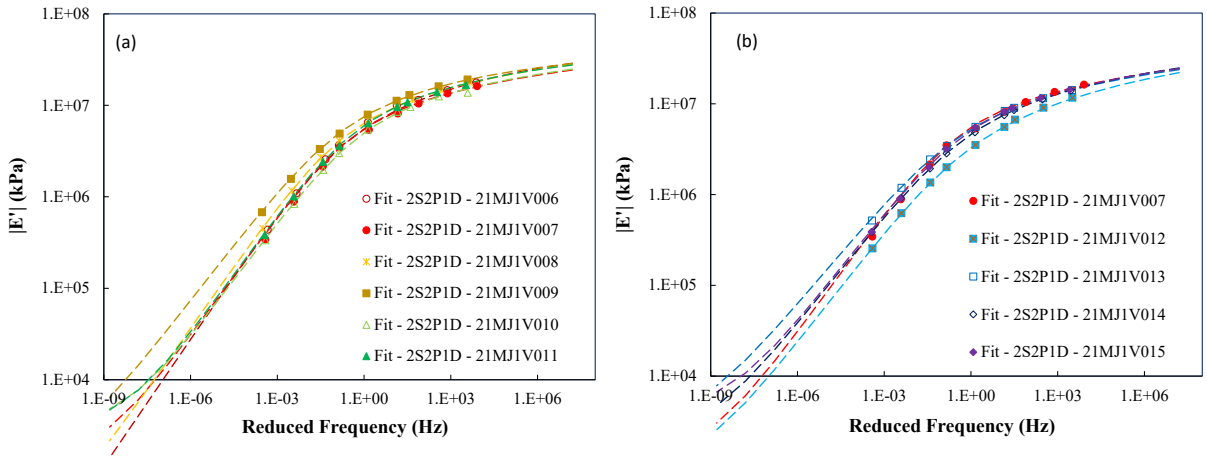

Figure 3.2 Dynamic modulus master curves of the testing samples in the MO 740 project: (a) Samples V006 – V011, the control mixture, (b) Samples V0012 – V015, the innovative mixtures with V007 control mix as a reference.

3.3. Cyclic Fatigue Testing Data of the MO 740 Project

The damage characteristic curves of all the samples are presented in Figures 3.3 and 3.4. In the plots, the curves generated from different specimens within one sample overlap with each other, which indicates the cyclic fatigue tests performed at S&T had low specimen-to-specimen testing variability. Figure 3.5 presents the comparison of the C vs. S curves among different samples and mixtures. According to Figure 3.5 (a), the C vs. S curves of different samples for the control mixture generally have the same shape and similar positions except for that of Sample V009. Note that Sample V009 also has the highest modulus from the dynamic modulus tests. The difference between damage characteristic curves of V009 and the other control sample can be attributed to the modulus difference since researchers have reported that stiffer mixtures tend to have C vs. S curves at high positions (Ding et al. 2020, Kim et al. 2022).

The C vs. S curves for different mixtures are compared in Figure 3.5 (b). The figure shows that the 50PE mixture has the highest damage characteristic curve and the 10ECR mixture has the lowest. Again, the observation is in line with the ranking of the mixture modulus. In fact, in the S-VECD model, a low C vs. S curve does not necessarily mean inferior fatigue performance. The fatigue failure is also dependent on the amount of damage that the material can carry before failure occurs. Therefore, another factor or a failure criterion has to be taken into account. Table 3.2 presents the values of the failure criterion parameter, D^R, of all the samples. The D^R parameter indicates the material's ductility. It varies between 0 and 1, and a higher D^R value means the material is more ductile (Wang and Kim 2017, Wang et al. 2021). According to Table 3.2, despite of the position of the C vs. S curves of the mixtures, all the modified mixes have higher D^R values than the control mixture. Among all the mixtures, the one with GTR has the highest ductility. Meanwhile, Mixture 50PE has slightly lower D^R value than Mixture 25PE, and the addition of RET in the 50PEL mixture significantly decreased the D^R value.

Given these factors, a fair comparison of the asphalt mixtures' fatigue performance should consider the mixture modulus, damage evolution curve, and the failure criterion. Those factors can be used together in the structural performance simulation in FlexPAVE™. Alternatively, the factors have also been integrated into one fatigue index parameter, S_{app}.

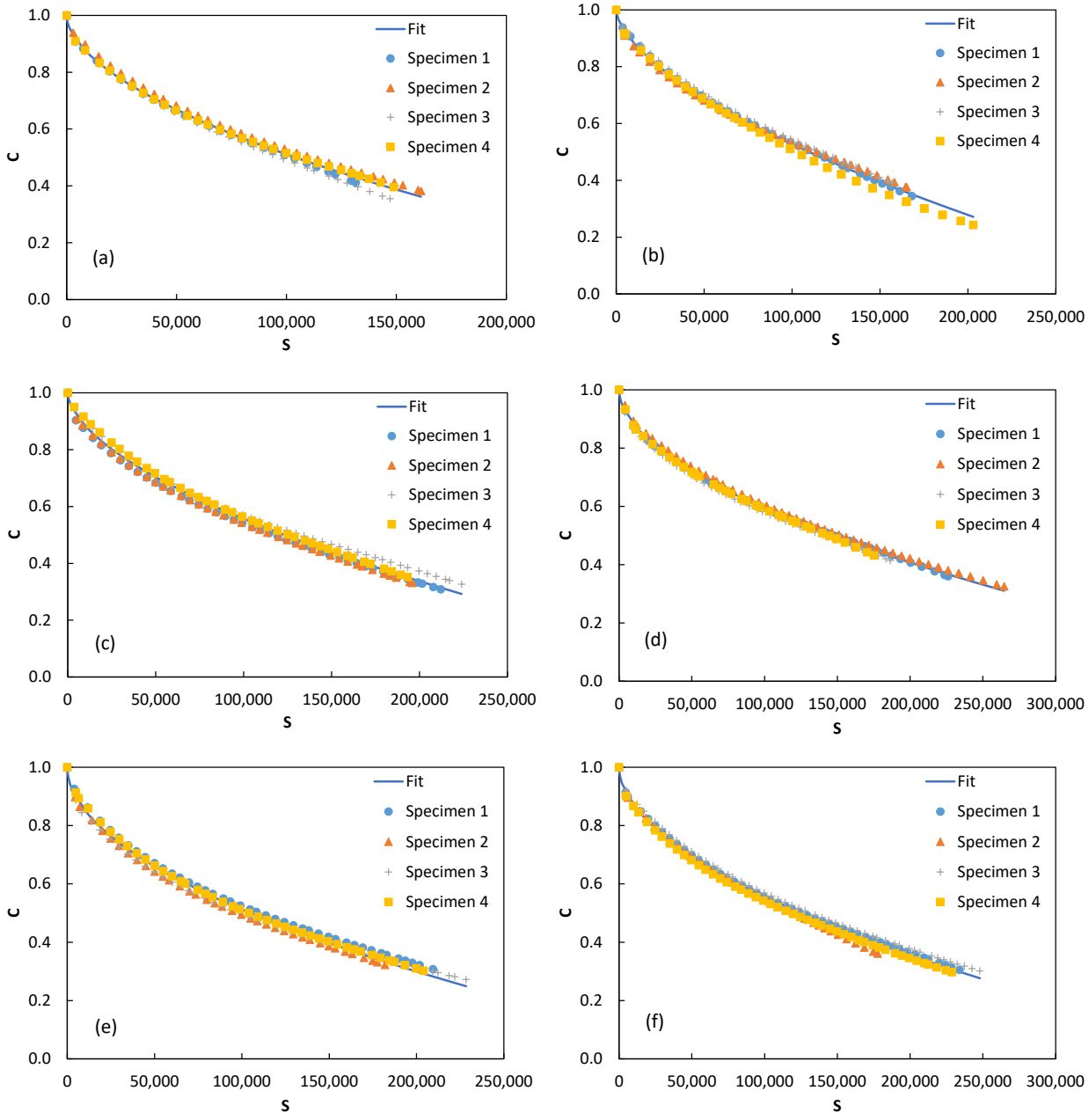

Figure 3.3 Damage characteristic curves of the samples for the control mixture: (a) – (f) Samples V006 – V011.

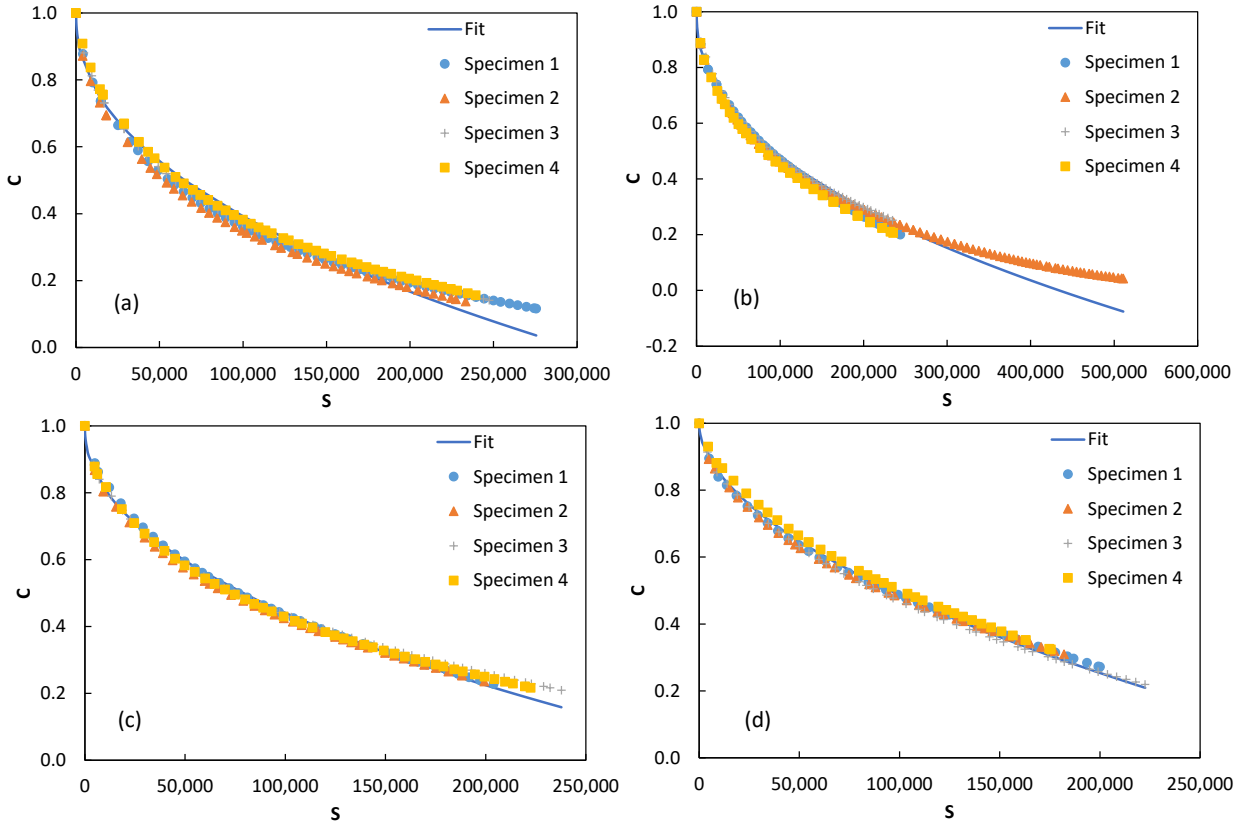

Figure 3.4 Damage characteristic curves of the testing mixtures: (a) Sample V012, 10ECR, (b) Sample V013, 50PE, (c) Sample V014, 25PE, and (d) Sample V015, 50PEL.

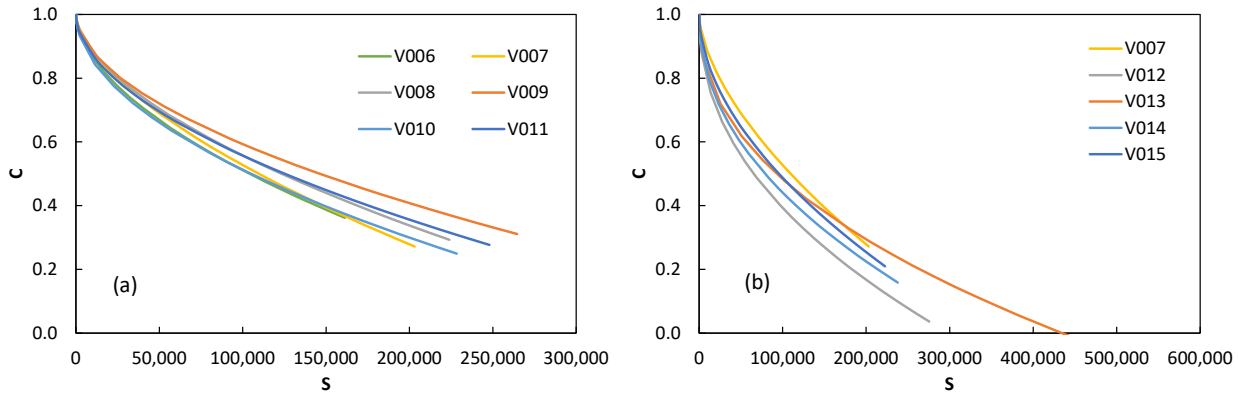

Figure 3.5 Comparison of the damage characteristic curves of all the testing samples: (a) samples for the control mix and (b) samples of the innovative mixtures with V007 Control as reference.

Table 3.2 Value of D^R as the Failure Criterion

Mix Type	Sample ID	D^R	Average
Control	V006	0.435	0.470
	V007	0.448	
	V008	0.473	
	V009	0.445	
	V010	0.532	
	V011	0.485	
10ECR	V012	0.766	0.766
50PE	V013	0.617	0.617
25PE	V014	0.628	0.628
50EPL	V015	0.541	0.541

3.4. Cracking Resistance Evaluation Using Index Parameter, S_{app}

As shown in Equation (2.3), the S_{app} index parameter integrates the mixture stiffness, damage characteristic curve, and failure criterion. The S_{app} values of all the samples are presented in Table 3.3. As shown in Table 3.3 and Figure 3.6, the 10ECR mixture has the highest cracking resistance. The addition of GTR dramatically increased the ductility of the mixture; thus, delaying the occurrence of macro cracking. Since 50PE and 25PE have similar D^R values, the slightly high modulus of the 50PE mixture can reduce the strain level generated under the same loading amplitude in pavement; therefore, yielding a better fatigue performance.

Table 3.3 Value of the Fatigue Index Parameter, S_{app}, of All the MO 740 Samples

Mix Type	Sample ID	S_{app}	Average
Control	V006	19.7	22.0
	V007	20.8	
	V008	24.3	
	V009	18.8	
	V010	25.0	
	V011	23.3	
10ECR	V012	45.5	45.5
50PE	V013	32.1	32.1
25PE	V014	26.4	26.4
50EPL	V015	21.8	21.8

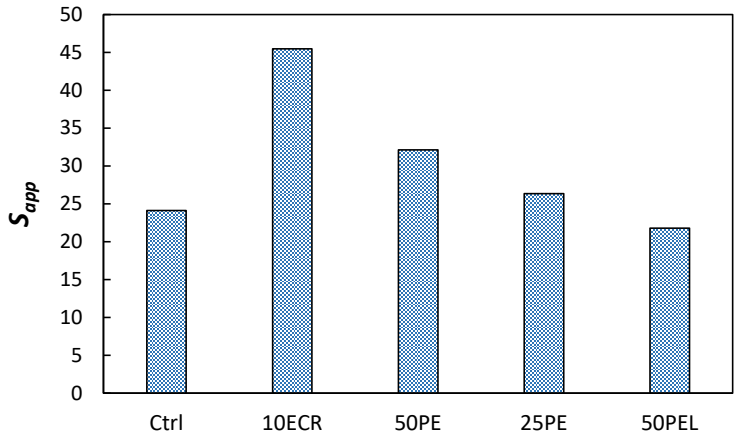

Figure 3.6 S_{app} values of the mixtures on MO 740.

3.5. Structural Performance Prediction Using FlexPAVE™

The obtained dynamic modulus and the S-VECD model coefficients of all the MO 740 samples were input into FlexPAVE™ for a full-scale structural performance simulation. The climate data in Columbia, MO was used. Since the pavement structure was a thin asphalt overlay over existing concrete layer and FlexPAVE™ does not model reflective cracking yet, the same pavement structure as shown in Figure 2.11 was used in this study. The predicted pavement performance is presented in Figures 3.7 and 3.8. As expected, the 10ECR section showed the best performance. Figure 3.9 presents the correlation between S_{app} and the predicted pavement damage at the end of design life. The correlation is high with R^2 value of 0.798. The relationship may vary as the pavement structure, climate, and traffic volume change in the simulation.

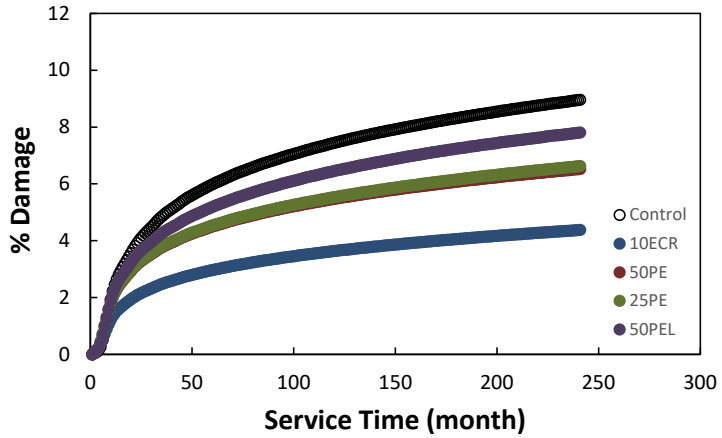

Figure 3.7 Damage growth of the pavement sections with different mixtures.

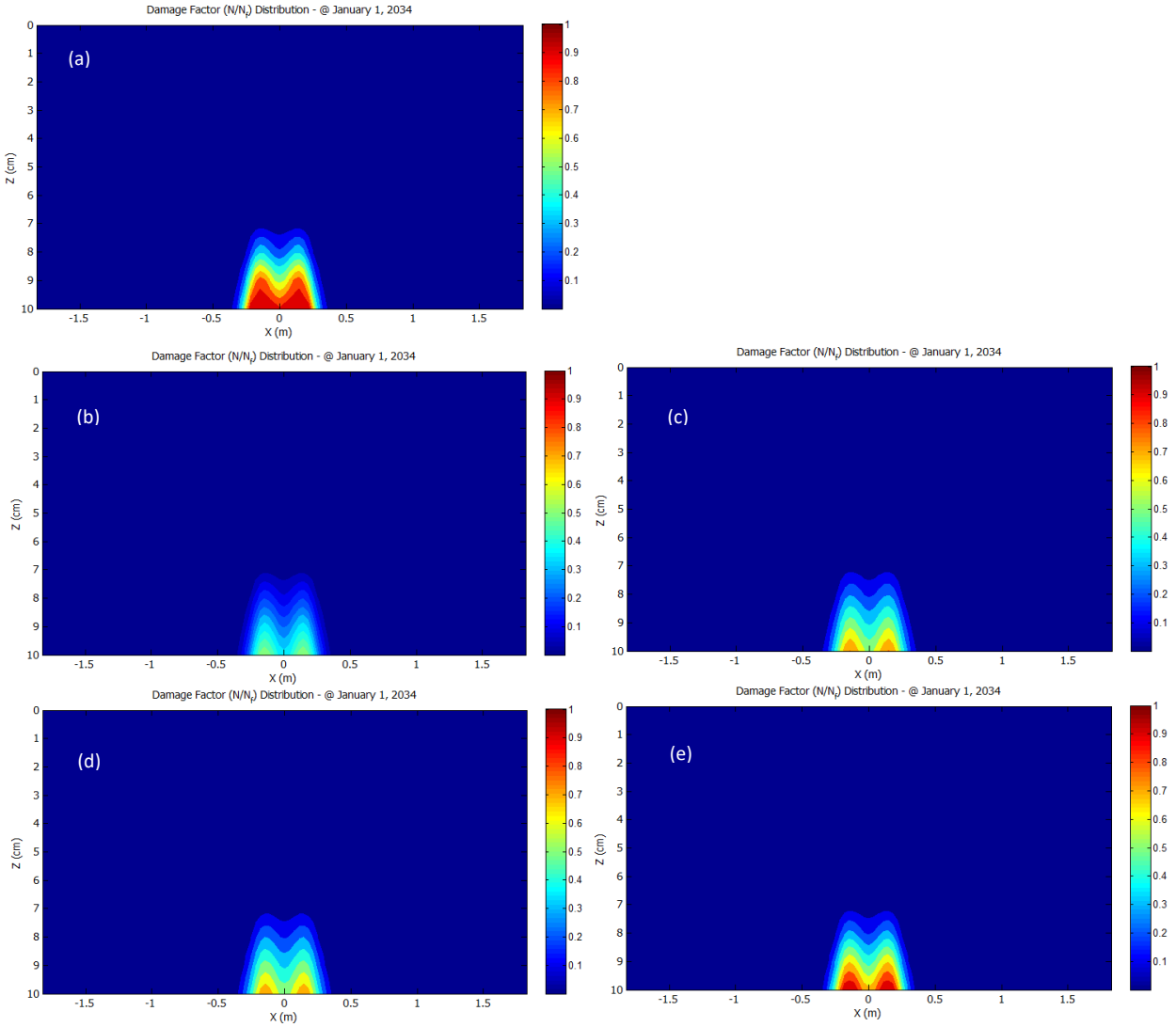

Figure 3.8 Damage contours in asphalt layer cross-sections with different mixtures: (a) Control, (b) 10ECR, (c) 50PE, (d) 25PE, and (e) 50PEL.

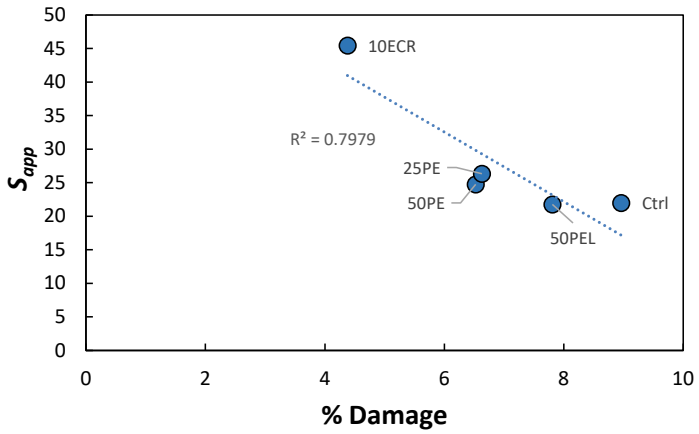

Figure 3.9 Correlation between S_{app} and %Damage at the end of pavement design life.

3.6. Data Analysis for AMPT Rutting Testing Results

Besides the dynamic modulus and cyclic fatigue tests, the rutting resistance was evaluated using the AMPT SSR test at S&T. The test was conducted as per AASHTO TP 134. For example, two specimens were at an intermediate temperature, and two were loaded at a high temperature. At each temperature, three deviatoric stress levels, i.e., 70 psi, 100 psi, and 130 psi, were applied with a confining pressure of 10 psi. The test generates a performance index called Rutting Strain Index (RSI). A high RSI value indicates the mixture may yield a high permanent strain under the same loading pattern; thus, a low RSI value is preferable (Kim et al. 2022, Wang et al. 2023). The RSI values of the tested samples are presented in Table 3.4. While the 10ECR mixture has the superior fatigue performance, it has the highest RSI value or the lowest rutting resistance. The 50PE mixture has the lowest RSI. The mixture stiffness may have played an important role in the mixtures' rutting resistance.

Table 3.4 RSI Values of All Testing Samples

Mix Type	Sample ID	RSI	Average
Control	V006	19.1	14.5
	V007	7.4	
	V008	10.2	
	V009	31.4	
	V010	9.2	
	V011	9.5	
10ECR	V012	16.5	16.5
50PE	V013	7.8	7.8
25PE	V014	10.2	10.2
50EPL	V015	8.4	8.4

3.7. Correlation Between AMPT Testing Results and Results from IDEAL-CT

Figure 3.10 presents the correlation between CT index and S_{app}. The CT values with reheated samples and production samples have been reported in Rath et al. (2022). It can be observed that only a weak correlation was found between CT with reheated samples and S_{app}. While other researchers have reported relatively good correlations between the two testing methods (Wang et al. 2023), the discrepancy could be due to the production, sampling, testing variability, and limited data points.

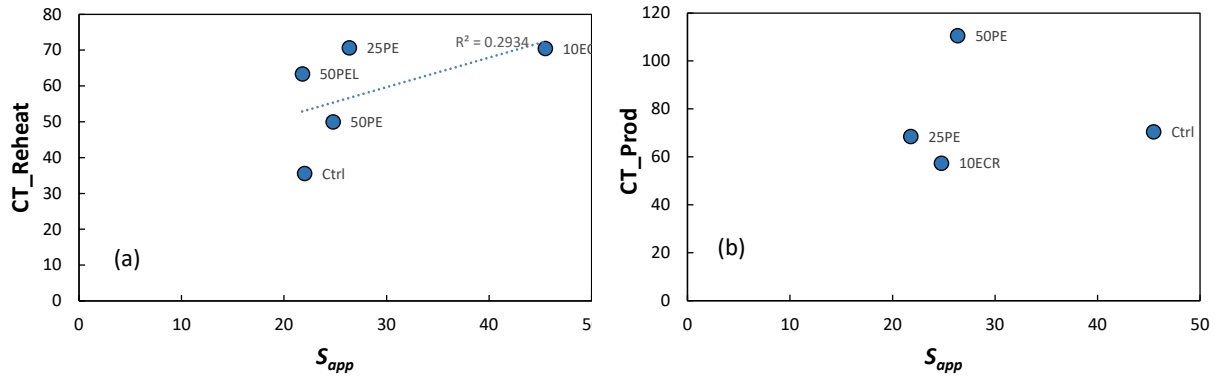

Figure 3.10 Correlation between the CT cracking index and S_{app}: (a) IDEAL-CT tests with reheated sample vs. S_{app} and (b) IDEAL-CT tests with samples compacted on site vs. S_{app}.

3.8. Summary

The AMAPT testing data on the MO 740 are analyzed and presented in this chapter. The tests included the AMPT dynamic modulus test, cyclic fatigue test, and the stress sweep rutting test. Five mixtures were evaluated, which are the control SP095C, mixture dry mixed with GTR, mixture with 0.50% polyethylene, mixture with 0.25% polyethylene, and mixture with 0.50% polyethylene and compatibilizer. The findings are summarized as follows.

- The variability in production of the control mixture were well controlled according to the measured dynamic modulus from different samples.
- The 50PE mixture has the highest modulus, and the 10ECR mix exhibited the lowest stiffness.
- The specimen-to-specimen testing variability in the cyclic fatigue was exceptionally low.
- The ranking of the positions of the C vs. S curves of different mixtures were in line with the ranking of their modulus. The damage characteristic curve alone may not tell the fatigue cracking resistance.
- The D^R failure criterion evaluates the mixture ductility. The 10ECR mixture has the highest D^R value, and the 50PEL has the lowest.

- The S_{app} index indicates the 10ECR mixture has the highest cracking resistance, and the trend in the structural simulation results is consistent with the index parameter.

- The RSI rutting index suggests the 10ECR has lowest rutting resistance while the 50PE mixture would yield the lowest permanent strain under the same level of repeated traffic load.

CHAPTER 4 COMPARISON BETWEEN FIELD OBSERVATION AND LABORATORY EVALUATION

Laboratory tests on the MO 740 mixtures were performed, and the results were presented in Chapter 3. The field performance of the test sections was collected in this chapter and used to evaluate the mix durability and the effectiveness of the laboratory tests.

4.1. Field Data Acquisition

Three methods were used to attempt to obtain the field performance of the test sections, including the video footage from the Automatic Road Analyzer (ARAN) provided by MoDOT, images from Google Earth, and street views from Google Maps.

4.1.1. Automatic Road Analyzer (ARAN)

MoDOT has been using ARAN to conduct pavement surveys. The video footage from ARAN survey on MO 740 was shared with S&T through an external secure channel for contractors. The user interface is shown in Figure 4.1. However, the videos shared with S&T only contained survey on discontinuous sections on the eastern part of Stadium Blvd and did not cover the test sections.

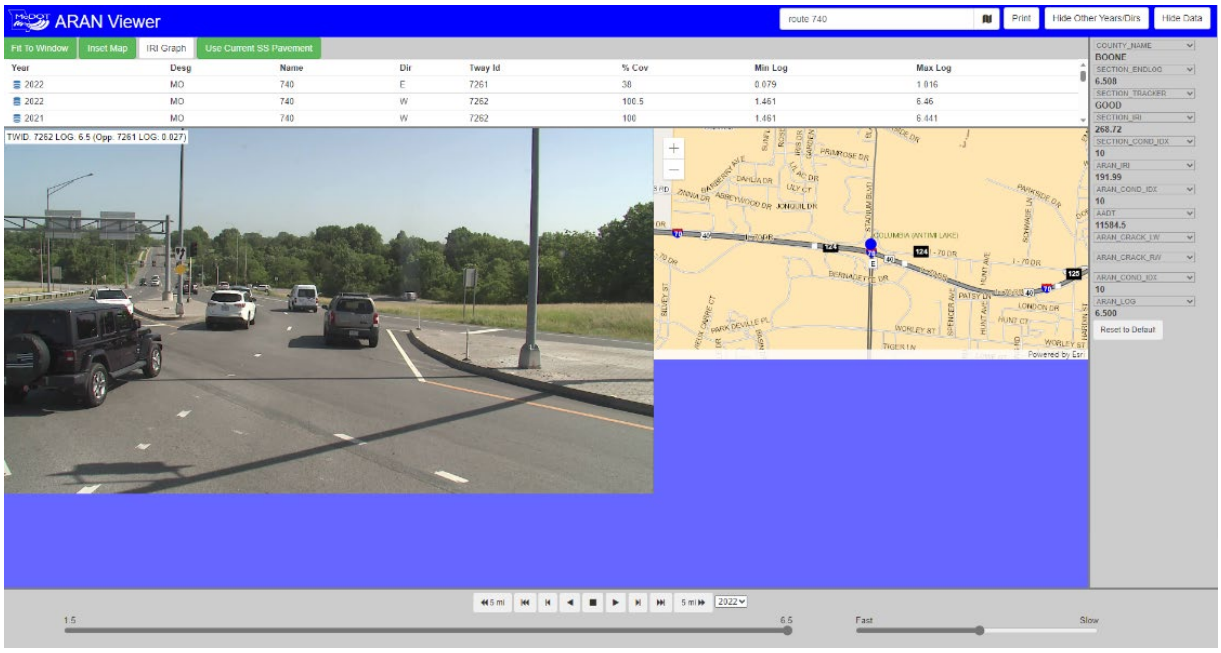

Figure 4.1 Interface of the ARAN Viewer.

4.1.2 Reflective Cracking based on Google Earth and Google Maps

Alternatively, street views from Google Earth and Google Maps were used in this study. The test sections on Google Earth and Google Maps are presented in Figures 4.2 and 4.3. While using

(a)

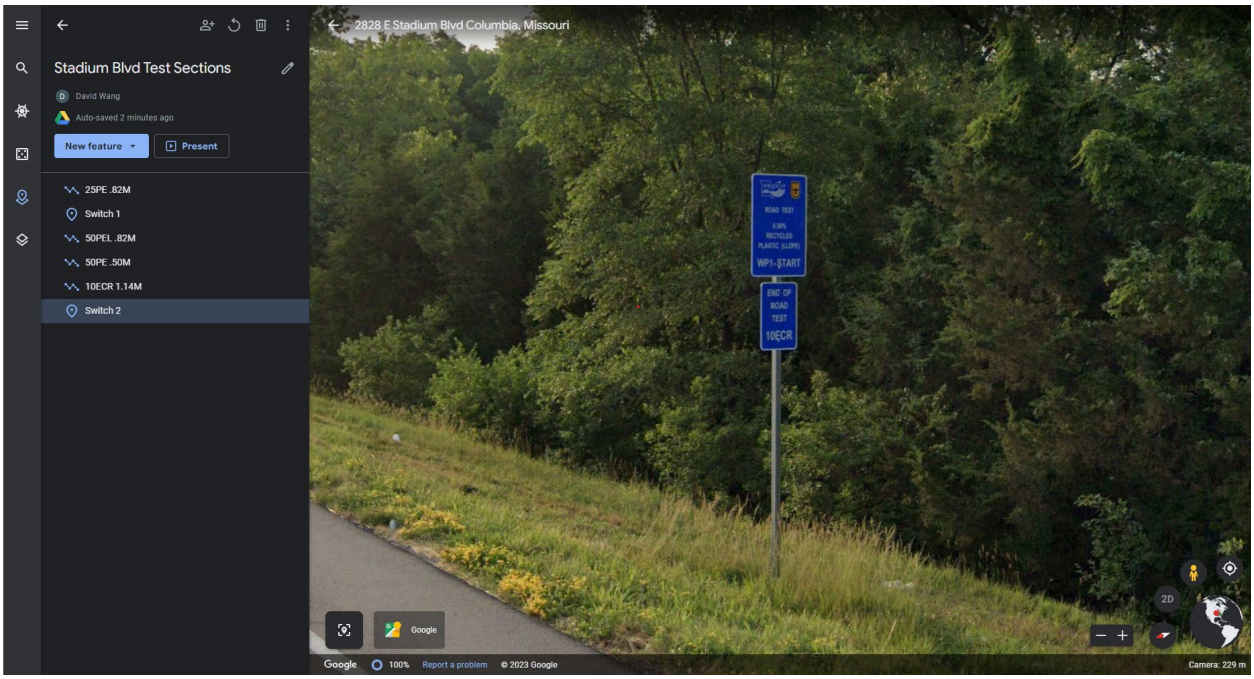

(b)

Figure 4.2 Stadium Blvd. on Google Earth: (a) location of the testing sections and (b) transection between two sections with a road sign specifying ‘End of Road Test, 10ECR.’

(a)

(b)

Figure 4.3 Stadium Blvd. street views on Google Maps: (a) one frame taken in 2019 with crack through all four lanes and (b) one frame on the same location taken in 2023 with crack propagated on only two lanes of the 10ECR section.

those tools, the researcher counted the number of cracks frame by frame along the test sections. In addition, the historical street view was also available on Google Maps. The numbers of reflective cracking in June 2023 (four years after traffic opening) and July 2019 (a few months before the resurfacing) were obtained. A new parameter called Cracking Reflection Rate was defined in this study. It is calculated as the ratio of the current number of cracking (2023) and number before construction (2019). In this way, the effect of unevenly distributed existing concrete joints or cracks was eliminated. The results are presented in Table 4.1 and Figure 4.4.

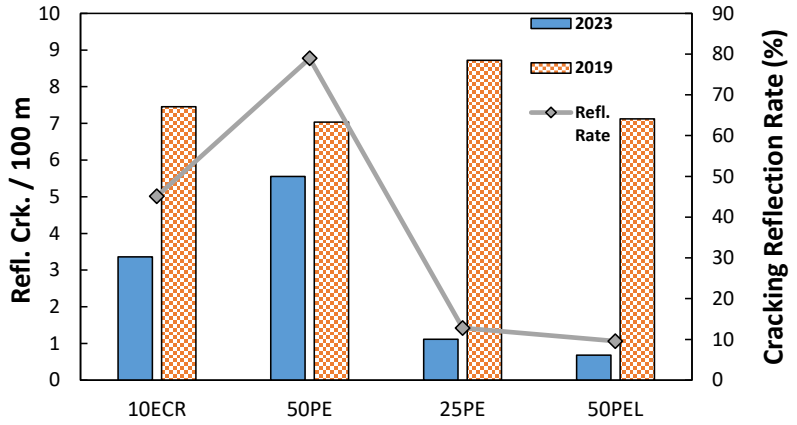

Figure 4.4 Number of reflective cracking per 100 m and reflection ratio on different test sections.

Table 4.1 Summary of Pavement Performance Regarding Reflective Cracking

Section	# Refl. Crk. /100 m (2019)	# Refl. Crk. /100 m (2023)	Cracking Reflection Rate (%)
Control	NA	NA	46
10ECR	7.45	3.36	45
50PE	7.04	5.56	77
25PE	8.73	1.13	12
50PEL	7.12	0.68	9

4.2. Comparison Between Field Observation and Laboratory Testing Results

The correlation between the field observation and the laboratory test results is presented in Figure 4.5. The result of direct comparison is not quite promising, neither for S_{app} nor the CT index. The variability in field tests is usually very high with many uncountable factors. For example, according to Rath et al. (2022), during the construction, some of the test sections were observed with a residual asphalt layer on the concrete after milling while others were not, as shown in Figure 4.6. Also, as the researcher conducted the survey, it was found that for the control section, the numbers of cracks on the eastbound and westbound directions were very different, which meant the traffic direction had a great impact of the pavement performance. Table 4.2 presents the information of the sections regarding the traffic direction and the

construction factor. In fact, none of the sections have the same condition; thus, they may not be the ideal sections for comparing mixture performance.

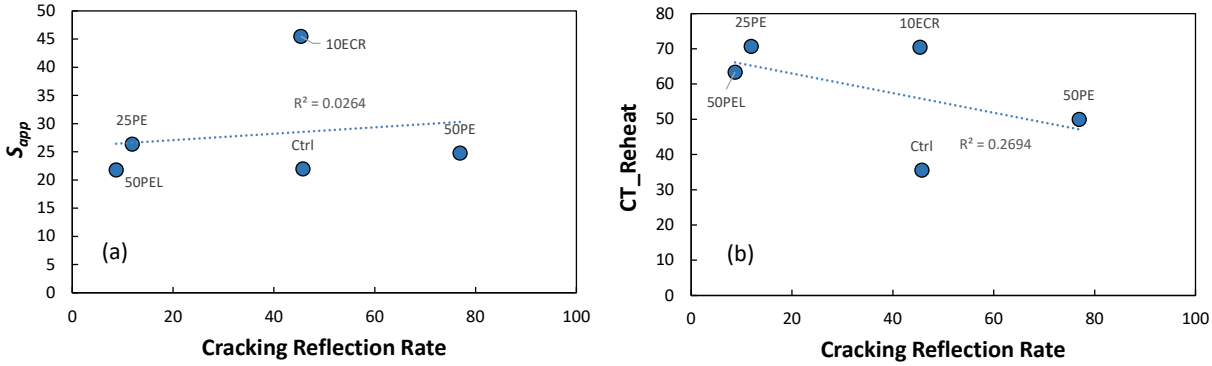

Figure 4.5 Correlation between cracking indices and cracking reflection rate: (a) S_{app} and (b) the CT index.

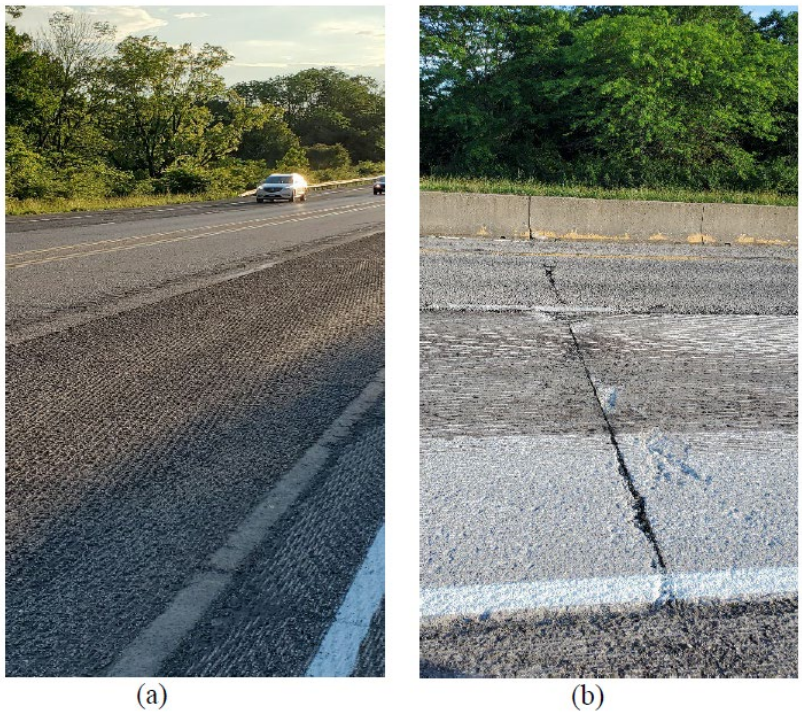

Figure 4.6 (a) Example of underlying asphalt pavement on the western-most stretch of the 50PEL and 10ECR sections, (b) Example of underlying concrete sections on rest of the project. (source: Rath et al. 2022)

Table 4.2 Characteristics of the Testing Sections

Characteristic	Eastbound	Westbound
With AC Residual	10ECR	50PEL
No AC Residual	50PE	25PE

Since the researchers discovered the traffic direction played an important role in the field performance, the sections were grouped by traffic directions, and performance was compared hereby within each group, as presented in Figure 4.7. It can be observed that on the eastbound direction sections, S_{app}, CT (reheated), and CT (production) exhibit the expected descending trend as the cracking reflection rate increases, and on the westbound sections, the trend is the opposite. Once the direction impact is eliminated, the index parameters from different testing methods are able to provide a consistent trend.

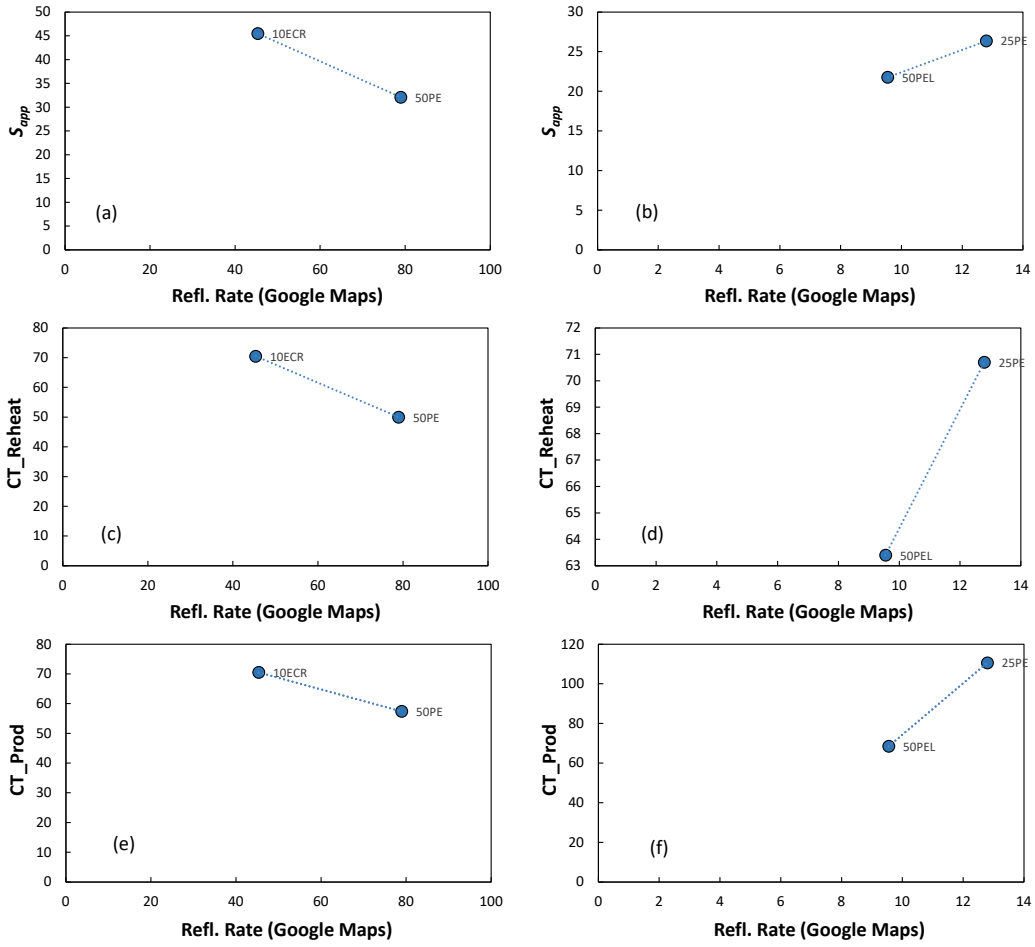

Figure 4.7 Correlation of cracking indices with cracking reflection ratio with separated directions: (a), (c), and (e) eastbound sections and (b), (d), and (f) westbound sections.

4.3. Summary

The field performance data were collected and compared with the laboratory testing results. The findings are summarized as follows.

- Three methods were used to acquire the number of reflective cracking in the field.
- The street view histories are available on Google Maps. A new parameter, Cracking Reflection Ratio, was defined by calculating the ratio of the current number of cracks and the number of cracks before construction. The parameter can eliminate the unevenly distributed existing joints and cracks for the short test sections.
- Each of the test sections has a unique characteristic in terms of the asphalt residual and the traffic direction. The traffic direction played an important role on pavement performance in this case. When the test sections with the same direction were compared, the same trend was provided by the AMPT cyclic fatigue test and the IDEAL-CT cracking test.

CHAPTER 5 CONCLUSION AND RECOMMENDATIONS

This study conducted a comprehensive analysis of the AMTP testing data from both the Highway 54 and MO 740 projects. The Highway 54 project contains data from ten asphalt samples that were acquired at different production times to evaluate production variability. The MO 740 project incorporates four innovative asphalt mixtures containing recycled plastic and ground tire rubber. Mix performance is assessed using the AMPT dynamic modulus test, cyclic fatigue test, and the SSR test. The testing results were compared with results from other testing methods and their field performance. The critical findings are summarized as follows.

- In the Highway 54 project, the dynamic modulus and fatigue testing results suggested that variability in production exists but was controlled in an acceptable range.

- The PVR function was successfully applied to the Highway 54 mixture. Using the PVR, the fatigue performance of mixtures produced for other sublots can be predicted once the volumetric information is measured during QA.

- In the MO 740 project, the mixture with 0.50% PE has the highest dynamic modulus while the mixture with GTR has the lowest dynamic modulus.

- Both the fatigue index and the pavement structural simulation results indicate that the GTR mixture is expected to have the highest cracking resistance.

- The RSI rutting index suggests the 10ECR mix has the lowest rutting resistance while the 50PE mixture would yield the lowest permanent strain under the same level of repeated traffic load.

- In terms of field evaluation, it was found that the consistency in design and construction of the test sections is extremely important. Once impacts of variables such as traffic direction is eliminated, different cracking testing methods are able to provide the same trend.

- As presented in Chapter 2, the volumetric parameters of asphalt mixtures can be strong indicators of their performance. However, because the volumetric information from the field samples only varied in a small range, it was difficult to develop solid pay factors for performance-related/based specifications. It is recommended that for future AMPT projects, testing samples are compacted at different air void levels to increase their range of variation so that a rigorous analysis can be conducted to develop the relationship between volumetric parameter and field performance. Such examples can be found in Jeong et al. (2020).

- As demonstrated in this study, investing in field testing can dramatically benefit the development and the application of new paving technologies. However, it is well known that field tests are subjected to high variability and unpredictable incidences. Therefore, it is important to design the field test sections with as many factors controlled as possible. An ideal testing location would have limited number of intersections, no or small grade,

no ramp, and consistent mainline traffic. Data obtained from well-controlled testing sections would be reliable; thus, maximizing the outcome from such investments.

- The data collected from the MO 740 project showed that there were some differences between the observed field performance and the expected performance based on the laboratory testing results. The discrepancy can be attributed to the unpredictable factors in the field and the different testing environments. Meanwhile, this observation also highlighted the importance of conducting field tests. It is recommended that, to apply new paving materials in the future, well-controlled field trial sections are constructed. Also, sufficient amount of mixture samples should be collected and stored so that laboratory tests using different testing methods and equipment can be conducted to fulfill future research needs.

- The study indicates that AMPT performance tests and their corresponding multi-scale models can capture not only the material performance, but also their fundamental material properties. The pavement life can be predicted accordingly. Such tests and analyses will help transportation engineers understand the material behavior and anticipate potential problems for future application of new paving materials.

REFERENCES

Ding, J., Wang. Y. D., Gulzar, S., Kim, Y.R., and Underwood, B. S. (2020). Uncertainty Quantification (UQ) of Simplified Viscoelastic Continuum Damage Fatigue Model using Bayesian Inference based Markov Chain Monte Carlo (MCMC) Method. *Transportation Research Record: Journal of the Transportation Research Board, Transportation*, Vol. 2674, Issue 4. DOI: 10.1177/0361198120910149.

Federal Highway Administration (FHWA) (2019). Cyclic Fatigue Index Parameter, S_{app}, for Asphalt Performance Engineered Mixture Design. *FHWA-HIF-19-091.* https://www.fhwa.dot.gov/pavement/pub_details.cfm?id=1098

Jeong, J., Wang, Y. D., Ghanbari, A., Nash, Casey, Nener-Plante, D., Underwood, B. S., and Kim, Y.R. (2020). Pavement performance predictions using performance-volumetric relationship and evaluation of construction variability: Example of Maine DOT shadow project for the development of performance-related specifications. *Construction and Building Materials*, Vol. 263. DOI: 10.1016/j.conbuildmat.2020.120150

Kim, Y. R., M. N. Guddati, Y. Choi, D. Kim, A. Norouzi, Y. Wang, B. Keshavarzi, M. Ashouri, A. Ghanbari, A. Wargo, and B. Underwood (2022). *Hot-Mix Asphalt Performance-Related Specification Based on Viscoelastoplastic Continuum Damage (VEPCD) Models*. Final Report. Federal Highway Administration. Publication No. FHWA-HRT-21-093.

Kim, Y. R., J. Lee, and Y. Wang (2015). *MEPDG Inputs for Warm-Mix Asphalts*. Final Report. NCDOT Project 2012-01, FHWA/NC/2012-01.

Rath, P., Meister, J., Arteaga-Larios, F., DuBois, C. J., Serrat, C., & Buttlar, W. (2022). Demonstration Project for Ground Tire Rubber and Post-Consumer Recycled Plastic-Modified Asphalt Mixtures. *Transportation Research Record*, 2676(7), 468-482. https://doi.org/10.1177/03611981221078844

Underwood, B.S., Baek, C., and Kim, Y.R. (2012). Simplified Viscoelastic Continuum Damage Model as Platform for Asphalt Concrete Fatigue Analysis. *Transportation Research Record: Journal of the Transportation Research Board*, 2296, 35–45.

Wang, Y. D., Ghanbari, A., Underwood, B. S., and Kim, Y. R. (2019). Development of a Performance-volumetric Relationship for Asphalt Mixtures. *Transportation Research Record: Journal of the Transportation Research Board*, Vol. 2673, Issue 6. DOI: 10.1177/0361198119845364

Wang, Y. D., Ghanbari, A., Underwood, B. S., and Kim, Y. R. (2020). Development of Preliminary Transfer Functions for Performance Predictions in FlexPAVE™. *Construction and Building Materials*, Vol. 266(B). DOI: 10.1016/j.conbuildmat.2020.121182

Wang, Y. D. Ghanbari, A., Underwood, B. S., and Kim, Y. R. (2021). Development of Performance-Engineered Mix Design for Asphalt Concrete. *International Journal of Pavement Engineering*. DOI: 10.1080/10298436.2021.1938044

Wang, Y. D., Keshavarzi, B., and Kim, Y. R. (2018). Fatigue Performance predictions of asphalt pavements using FlexPAVE™ with the SVECD model and D^R failure criterion. *Transportation Research Record: Journal of the Transportation Research Board*, Vol. 2672, Issue 40. DOI: 10.1177/0361198118756873

Wang, Y. and Kim, Y. R. (2017). Development of a pseudo strain energy-based fatigue failure criterion for asphalt mixtures. *International Journal of Pavement Engineering*. DOI: 10.1080/10298436.2017.1394100

Wang, Y. D., Liu, J. and Liu, J. (2023) Integrating Quality Assurance in Balance Mix Designs for Durable Asphalt Mixtures: State-of-the-Art Literature Review, *ASCE Journal of Transportation Engineering Part B: Pavements*. Vol. 149, Issue 1. DOI: 10.1061/JPEODX.PVENG-957

Wang, Y., Norouzi, A. H., and Kim, Y. R. (2016). Comparison of Fatigue Cracking Performance of Asphalt Pavements Predicted by Pavement ME and LVECD Programs. *Transportation Research Record: Journal of the Transportation Research Board*, Vol. 2590, pp. 44-55, DOI: 10.3141/2590-06

Wang, Y. D., Underwood, B. S., and Kim, Y. R. (2020). Development of Fatigue Index Parameter, S_{app}, for Asphalt Mixes Using Viscoelastic Continuum Damage Theory. *International Journal of Pavement Engineering*. DOI: 10.1080/10298436.2020.1751844.

APPENDIX A Statistical Analysis of Dynamic Modulus Testing Results of HWY 54 Project

Table A Precision for Dynamic Modulus

Sample ID	Temp.	Rep.1	Rep.2	Rep.3	Rep.4	Average |E*|	Repeatability Coefficient of Variation for |E*|	Sr
	°C	MPa	MPa	MPa	MPa	MPa	%	%
040	4.2	14880.0	14850.0	15109.0	14839.0	14919.5	4.4	6
	20.2	6928.0	4973.0	6894.0	6628.0	6355.8	5.3	7
	40.1	1360.0	1320.0	1410.0	1313.0	1350.8	7.4	9
041	4.2	13681.0	14646.0	14769.0	13242.0	14084.5	4.5	6
	20.2	6505.0	5977.0	6918.0	6206.0	6401.5	5.3	7
	40.1	1127.0	1217.0	1383.0	1235.0	1240.5	7.5	9
042	4.2	14896.0	14766.0	14877.0	14991.0	14882.5	4.4	6
	20.2	7281.0	6811.0	7385.0	7256.0	7183.3	5.2	7
	40.1	1445.0	1373.0	1526.0	1484.0	1457.0	7.3	9
043	4.2	16305.0	16366.0	15896.0	15740.0	16076.8	4.4	6
	20.2	8165.0	8572.0	8271.0	7968.0	8244.0	5.0	7
	40.1	1866.0	2005.0	1869.0	1800.0	1885.0	6.9	9
044	4.2	12723.0	12969.0	13242.0	12268.0	12800.5	4.6	6
	20.2	5786.0	5927.0	5600.0	5427.0	5685.0	5.5	7
	40.1	1047.0	1105.0	1110.0	1042.0	1076.0	7.8	9
045	4.2	14072.0	14791.0	13418.0	15407.0	14422.0	4.5	6
	20.2	6720.0	6856.0	6378.0	7392.0	6836.5	5.2	7
	40.1	1266.0	1305.0	1132.0	1500.0	1300.8	7.5	9
046	4.2	9215.0	8666.0	9295.0	8764.0	8985.0	4.9	7
	20.2	3743.0	3702.0	3803.0	3662.0	3727.5	6.0	8
	40.1	752.1	748.1	768.9	700.1	742.3	8.4	11
047	4.2	11651.0	12167.0	11424.0	11830.0	11768.0	4.7	6
	20.2	5804.0	5852.0	5488.0	6106.0	5812.5	5.4	7
	40.1	1394.0	1448.0	1343.0	1484.0	1417.3	7.3	9
048	4.2	11298.0	11838.0	11020.0	11629.0	11446.3	4.7	6
	20.2	5122.0	5291.0	4994.0	5332.0	5184.8	5.6	7
	40.1	1094.0	1098.0	1057.0	1107.0	1089.0	7.7	9
049	4.2	11699.0	11906.0	11705.0	11739.0	11762.3	4.7	6
	20.2	5719.0	5615.0	5834.0	5562.0	5682.5	5.5	7
	40.1	1094.0	1221.0	1101.0	1231.0	1161.8	7.6	9

Table B Precision for Phase Angle

Sample ID	Temp.	Rep.1	Rep.2	Rep.3	Rep.4	Average Phase Angle	Repeatability Coefficient of Variation for Phase Angle	Sr
	°C	°	°	°	°	°	%	%
040	4.2	8.4	8.8	8.7	8.9	8.7	0.6	0.6
	20.2	19.3	19.7	19.5	19.2	19.4	0.8	0.7
	40.1	36.5	36.1	34.5	36.3	35.9	1.1	1.1
041	4.2	8.7	8.6	6.7	8.3	8.1	0.6	0.6
	20.2	34.1	21.8	18.3	18.4	23.1	0.8	0.7
	40.1	38.1	37.5	36.3	34.5	36.6	1.1	1.1
042	4.2	8.3	8.5	9.1	8.3	8.5	0.6	0.6
	20.2	17.2	16.9	17.1	17.1	17.1	0.7	0.7
	40.1	35.5	35.0	35.5	35.8	35.4	1.1	1.1
043	4.2	7.7	7.5	7.7	7.5	7.6	0.6	0.6
	20.2	14.1	15.3	15.1	15.6	15.0	0.7	0.7
	40.1	31.9	32.0	32.7	32.5	32.3	1.0	1.1
044	4.2	9.2	9.4	9.1	8.9	9.1	0.7	0.6
	20.2	19.2	19.3	19.4	19.5	19.3	0.8	0.7
	40.1	36.2	35.6	34.0	36.8	35.6	1.2	1.1
045	4.2	8.5	8.4	8.9	8.4	8.5	0.6	0.6
	20.2	18.2	18.6	18.3	18.5	18.4	0.8	0.7
	40.1	37.3	37.6	33.1	37.0	36.2	1.1	1.1
046	4.2	10.6	11.5	10.4	10.2	10.7	0.7	0.7
	20.2	20.8	19.1	17.9	20.1	19.5	0.9	0.9
	40.1	35.5	33.5	33.6	34.0	34.1	1.3	1.3
047	4.2	8.9	8.3	8.8	8.4	8.6	0.7	0.6
	20.2	16.3	17.2	16.4	16.4	16.6	0.8	0.7
	40.1	30.9	31.2	29.3	31.4	30.7	1.1	1.1
048	4.2	9.8	9.7	9.9	8.8	9.5	0.7	0.6
	20.2	18.7	19.1	18.7	19.2	18.9	0.8	0.7
	40.1	33.9	33.9	33.7	33.2	33.7	1.2	1.1
049	4.2	8.8	9.2	6.2	8.8	8.2	0.7	0.6
	20.2	18.4	17.4	18.2	17.4	17.9	0.8	0.7
	40.1	33.5	34.5	33.3	34.2	33.9	1.1	1.1